



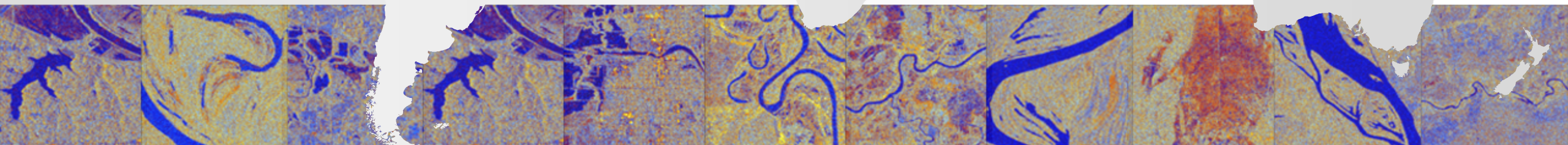
IMPROVING SEMANTIC WATER SEGMENTATION BY FUSING SENTINEL-1 INTENSITY AND INTERFEROMETRIC SYNTHETIC APERTURE RADAR (INSAR) COHERENCE DATA

by
Ernesto Colon

Advisor: Sam Keene

The Cooper Union for the Advancement of Science and Art
Albert Nerken School of Engineering

April 12th, 2022



AGENDA

- Introduction
 - Motivation
 - Previous works
 - Problem statement
- Background
 - Microwave remote sensing
 - SAR and InSAR
- Data processing and augmentation
- Models and methodology
- Results
- Conclusion
- Q&A



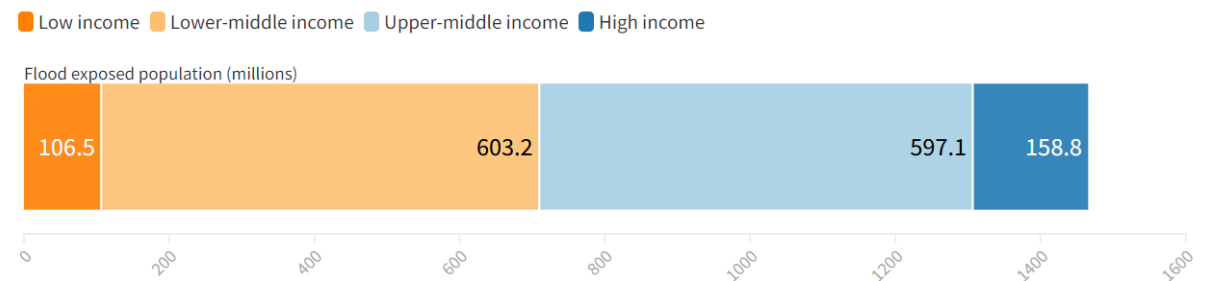
THE COOPER UNION

MOTIVATION

- **Why should we improve semantic water segmentation for flood mapping?**
- The latest Intergovernmental Panel on Climate Change (IPCC) report estimates that “50 to 75% of the global population could be exposed to periods of life-threatening climatic conditions due to extreme heat and humidity by 2100.” [1][2]

MOTIVATION

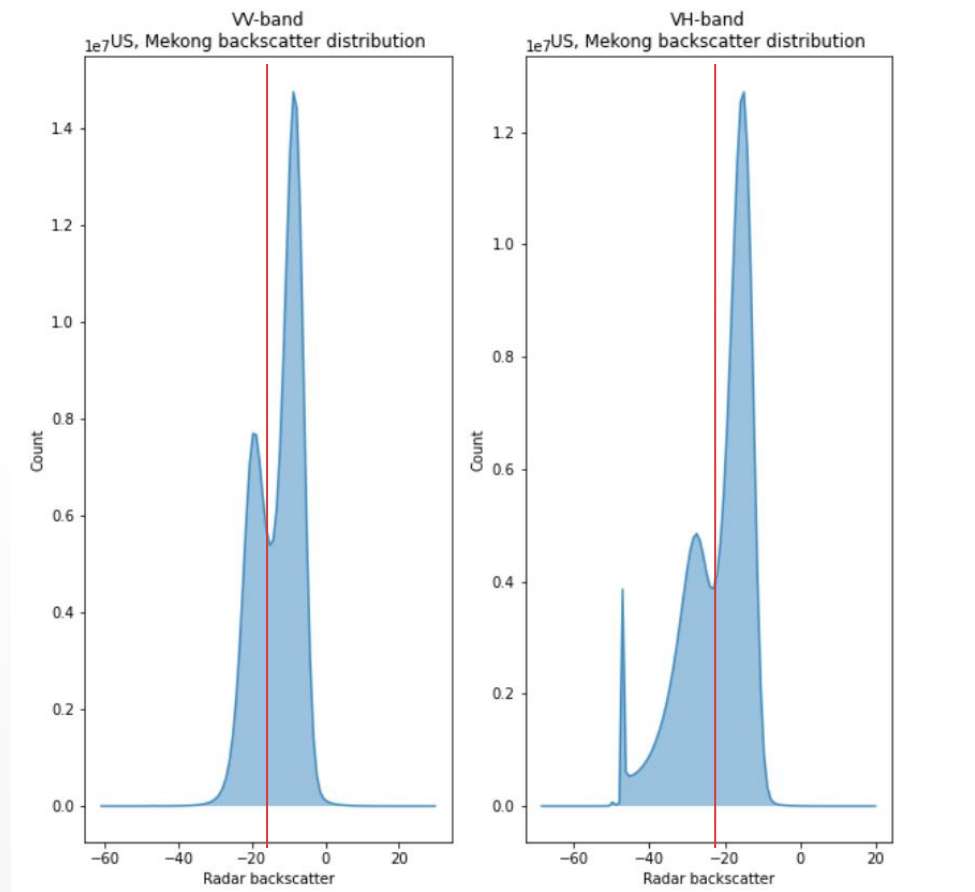
- The World Bank estimates that close to 1.5 billion people are exposed to the risk of flooding worldwide. Moreover, up to 89% of the exposed population live in low- and middle-income countries [3][4]
- Extreme flooding events perpetuate economic hardships and cost lives [3][4]
- **We cannot prevent an extreme flooding event, but we can be proactive and prepare**



Flood exposed population (millions), by income group. Adapted from [3][4]

MOTIVATION AND PREVIOUS WORK

- Synthetic Aperture Radar (SAR) **backscatter intensity** has been used extensively for surface water mapping
- Expert methods include:
 - Otsu thresholding [5][6]
 - HydroSAR [7][8][9][10]
 - Threshold → HAND layer → Fuzzy logic
 - HYDRAFloods [11]



Sentinel-1 backscatter bi-modal distributions for VV and VH polarized bands over the Mekong region. Sentinel-1 data processed with Python.

MOTIVATION AND PREVIOUS WORK

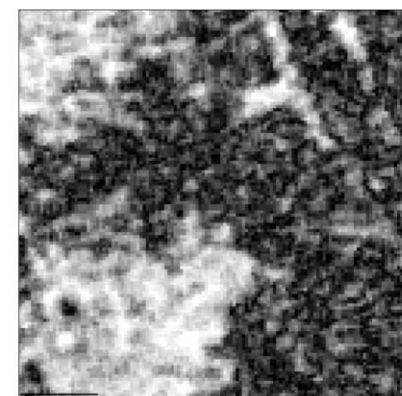
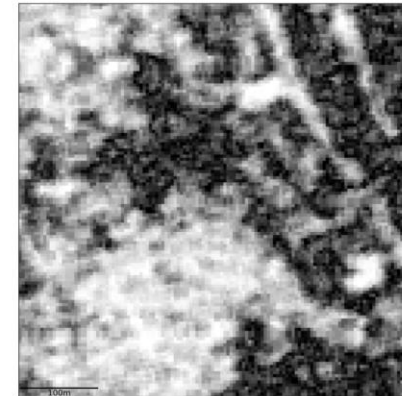
- Recently, machine learning techniques have gained increased popularity for flood mapping applications
- Some examples include:
 - Semantic segmentation using SAR backscatter intensity [12][13][14][15]
 - Segmentation combining SAR backscatter intensity and coherence [16][17][18][19]
 - Most studies are limited to a few case studies and/or use private data

PROBLEM STATEMENT

- In this study 10-meter resolution **Sentinel-1 backscatter intensity and InSAR coherence data is fused across geographically diverse regions** for semantic water segmentation
- Uni- and bi-temporal classification **models are cross-trained using optically derived Sentinel-2 water masks**
- This study is focused on the relative improvement gained by adding the coherence data to the intensity data
- Inspired by the Sen1Floods11 team's work [13][27]

WHY COHERENCE?

- When flooding occurs, stagnant water changes the spatial distribution of scatterers on the surface
- We exploit the **spatial decorrelation** as a signal for semantic segmentation



Pre-event intensity (VV) and coherence (top), co-event intensity (VV) and coherence (bottom). Sentinel-1 data processed by GEE [28], ASF [10] and Python.

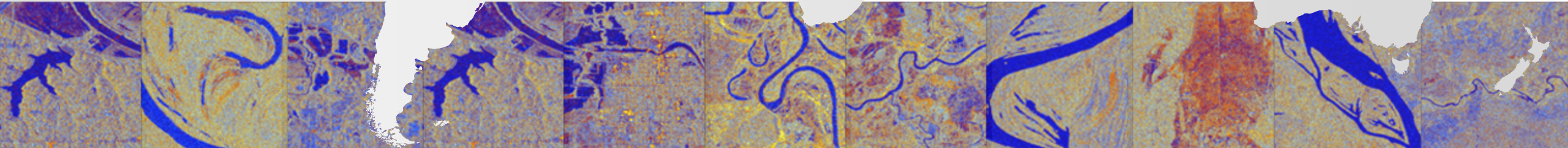


THE COOPER UNION



A bit of background on

MICROWAVE REMOTE SENSING



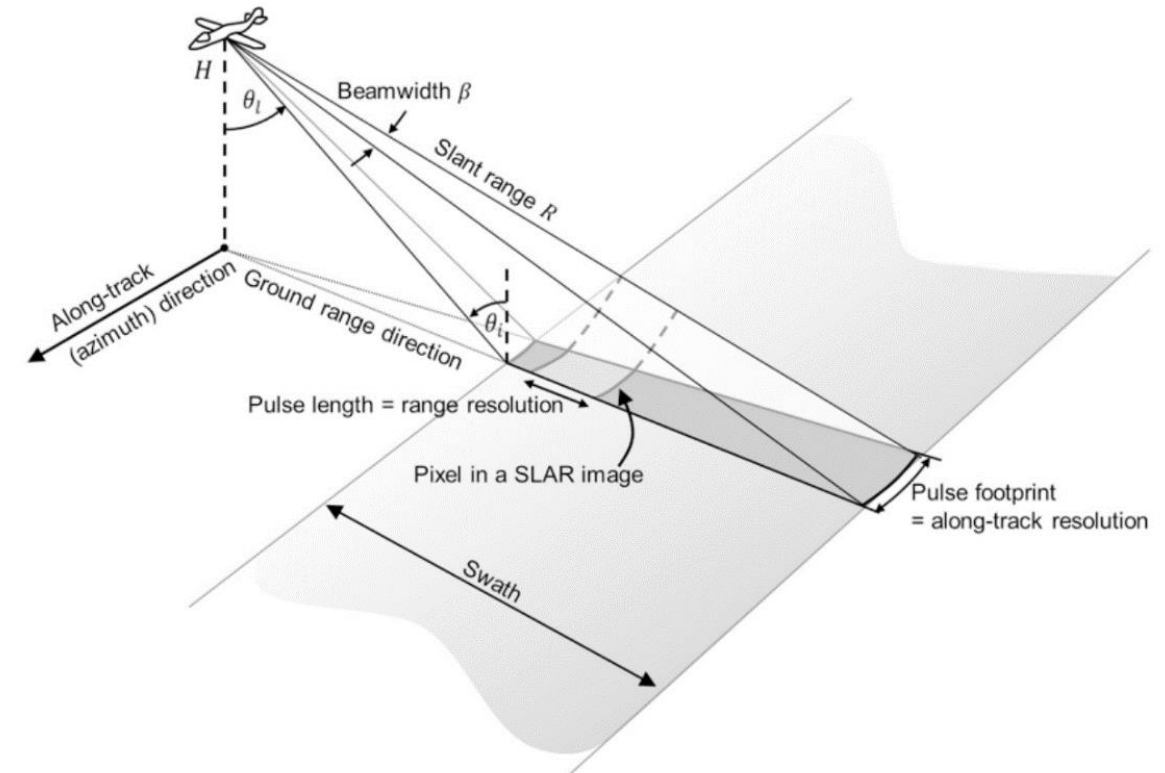
MICROWAVE REMOTE SENSING

- Microwave remote sensors can be active or passive
 - Passive examples:
 - Radiometers
 - Active examples:
 - Synthetic Aperture Radar (SAR)
 - Altimeters
- Advantages
 - Sense through clouds
 - Weather independent
 - All day and night operation
 - Complementary to optical remote sensors

SIDE-LOOKING AIRBORNE RADAR (SLAR) IMAGE FORMATION

- As the radar platform flies in the azimuth direction, we process the radar echoes and form a 2D image
- Each radar pixel is a complex quantity
 - We can exploit both magnitude and phase information
- **Problem:** the azimuth resolution depends on the antenna's beam width

$$\rho_{az} = \frac{\lambda}{L} R = \beta R [m]$$

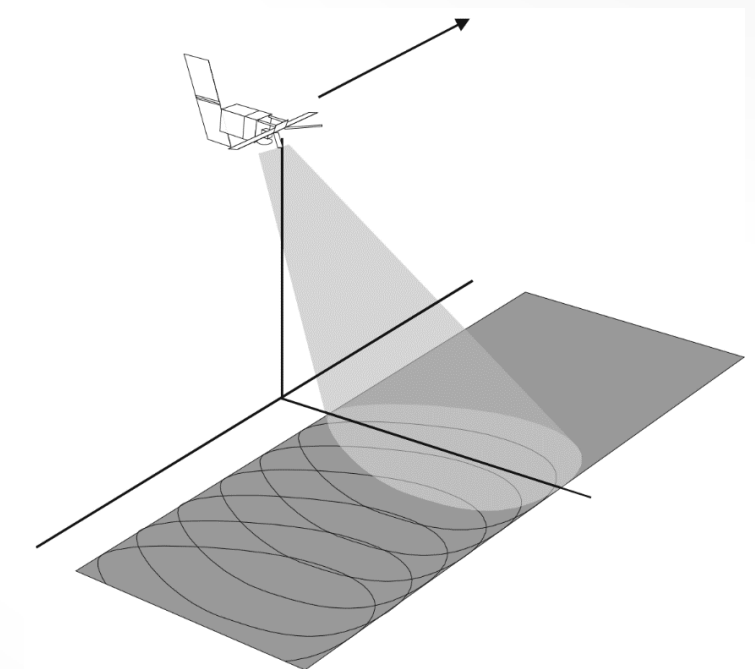
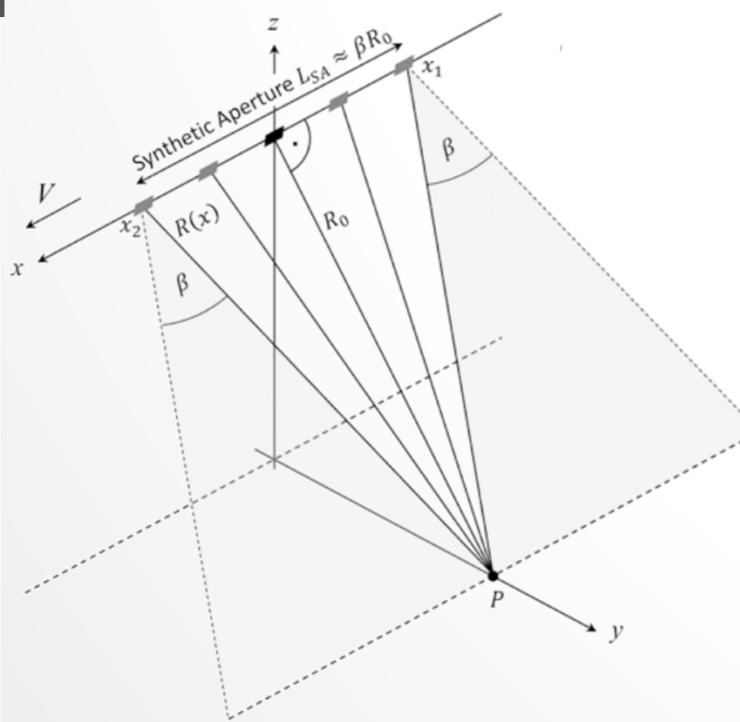


Side-looking Airborne Radar (SLAR) viewing geometry. Adapted from [21]

SYNTHETIC APERTURE RADAR (SAR)

- A SAR platform synthesizes a larger equivalent antenna from a physically shorter antenna
- Radar cross-section

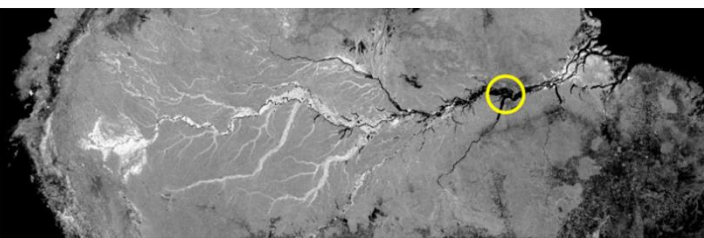
$$\sigma_0 = \frac{P_r (4\pi)^3 R^4}{AP_t G^2 \lambda^2}$$



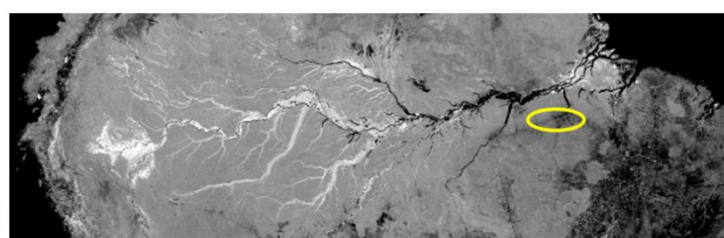
Synthetic Aperture Radar (SAR) viewing geometry. Adapted from [21] (left) and [22] (right)

EXAMPLES OF RADAR BACKSCATTER

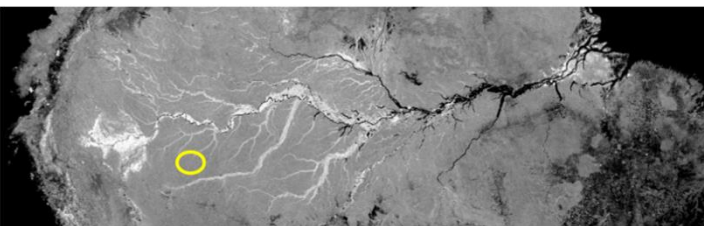
Specular Reflection



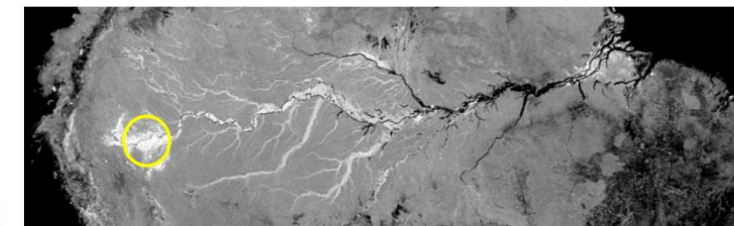
Rough Surface Reflection



Volume Scattering by Vegetation



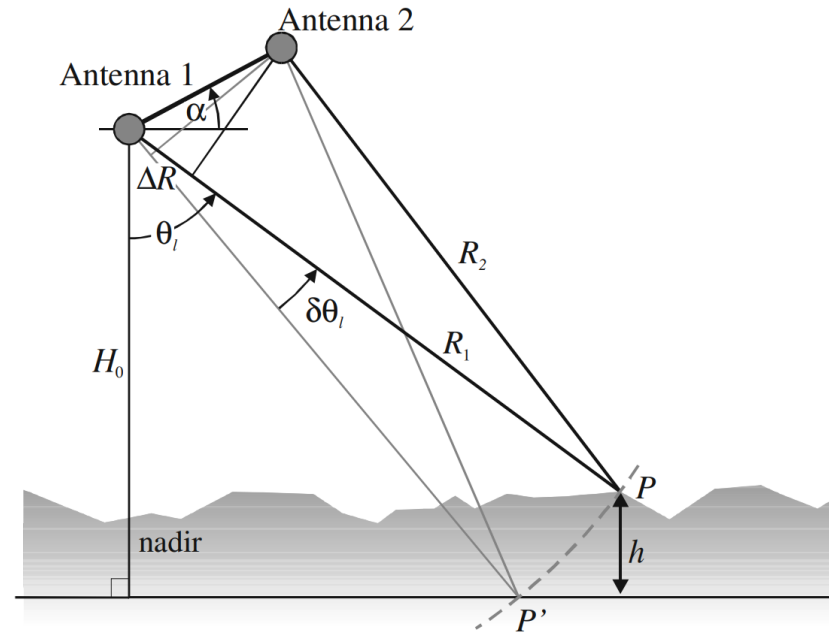
Double Bounce



Examples of backscatter and gray level intensity. Image adapted from [20]

INTERFEROMETRIC SAR

- Repeat-pass interferometry
 - Two observations made from the same location in space, but at different times
 - **Interferometric phase is proportional to any change in the range of a surface feature directly [20]**

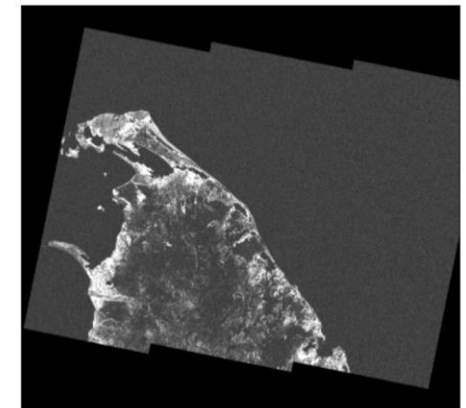
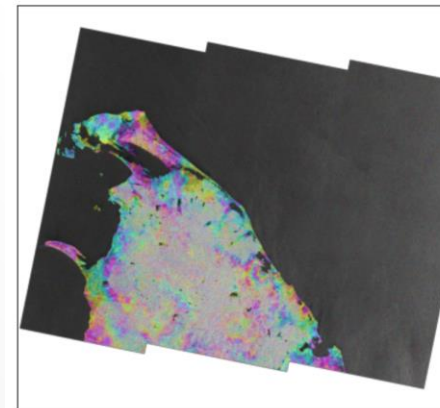
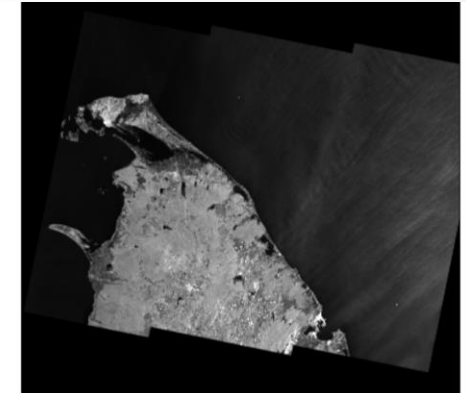
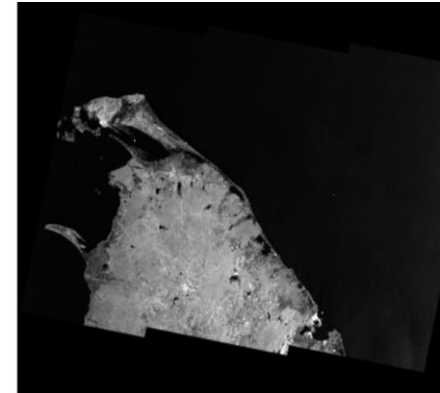


Geometry for interferometry. Adapted from [22]

INTERFEROMETRIC COHERENCE MAGNITUDE

- Coherence is a measure of how similar two waves are
- Interferometric coherence is the complex cross-correlation of two SAR acquisitions

$$|\gamma[i, k]| = \frac{|\sum_N u_1[i, k]u_2^*[i, k]|}{\sqrt{\sum_N |u_1[i, k]|^2 \sum_N |u_2[i, k]|^2}}$$



Interferogram over Sri-Lanka. Primary image date: May 12th (top-left), secondary image date (top-right): May 24th 2017, interferogram (bottom-left), and coherence map (bottom-right). Sentinel-1 data processed by ASF [10]

INTERFEROMETRIC COHERENCE DECORRELATION

- Some sources of decorrelation include [22]:
 - Baseline decorrelation
 - Temporal decorrelation
 - Volume decorrelation
 - Landscape changes (e.g., flooding)



DATA PROCESSING AND PREPARATION

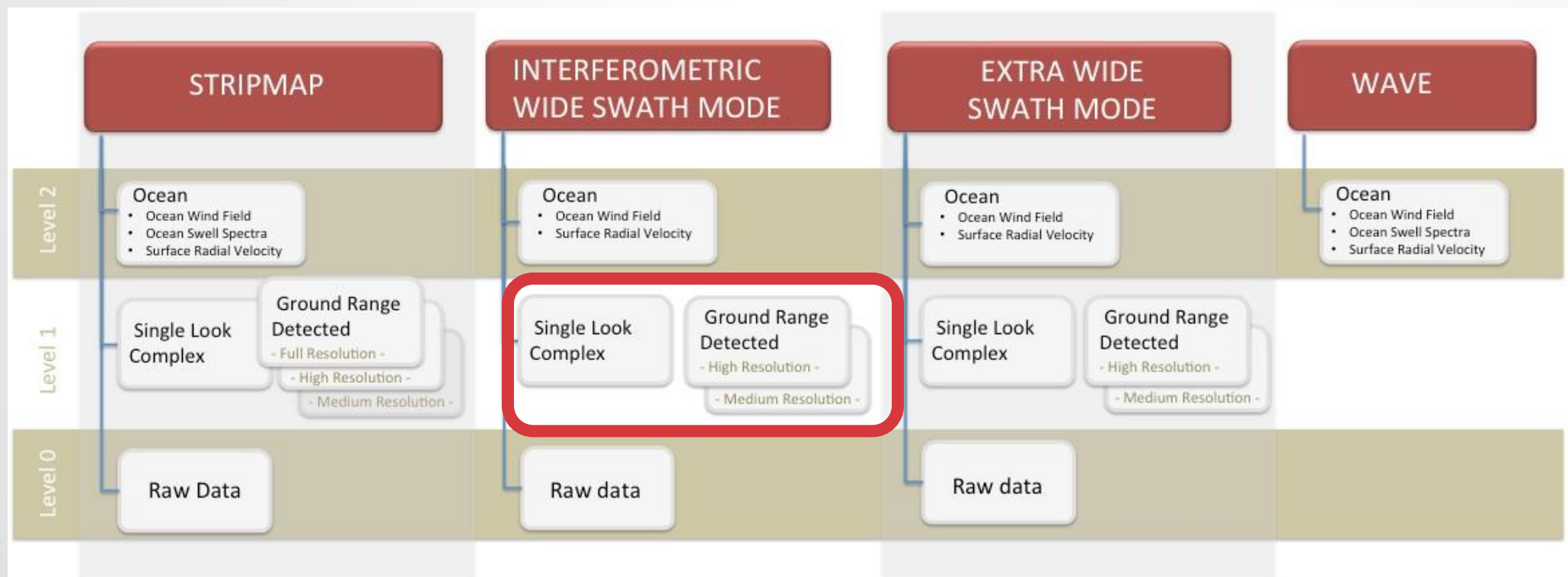
COPERNICUS SENTINEL-1

- Mission comprised of twin satellites (Sentinel-1A and 1B)
- C-band sensor with dual-polarization (VV+VH, HH+HV, HH, VV)
- 6-day repeat cycle
- Open data access
- Spatial resolution as high as 10-meter per pixel [25]



Image taken from:
<https://sentinels.copernicus.eu/web/sentinel/missions/sentinel-1/overview>

COPERNICUS SENTINEL-1



Copernicus Sentinel-1 core products. Adapted from [26]

SOME DEFINITIONS

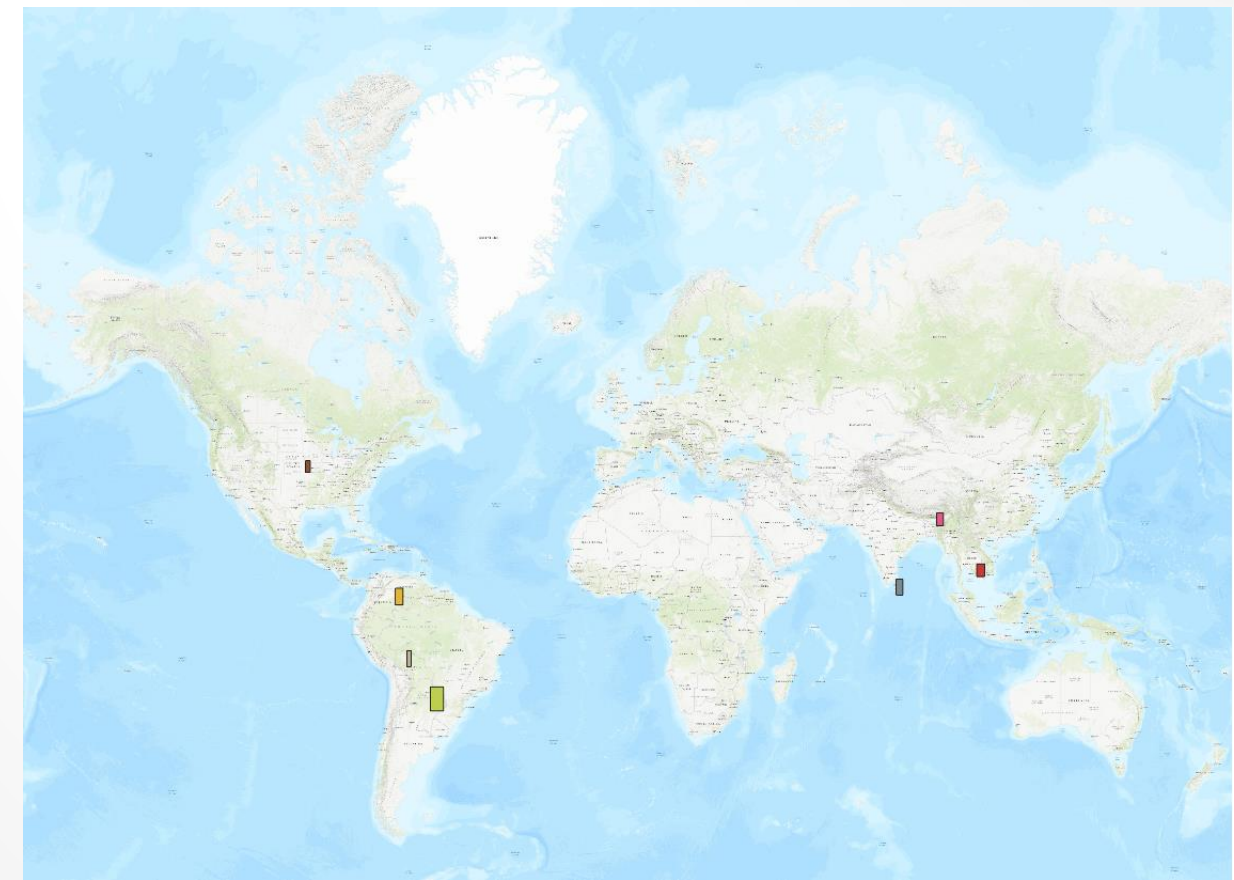
- Temporal definitions
 - Co-event means 'during' the flooding event
 - Pre-event means 'prior' to the flooding event

SEN1FLOODS11 DATA SET

- A georeferenced SAR intensity (VV, VH) data set generated by Cloud to Street [13][27]
- 11 flood events between 2016 and 2019 across the world
- Data set contains classified permanent water, flood water, and Sentinel-1 backscatter intensity at 10-m resolution
- 4,831 chips (512 x 512) with 446 hand-labeled and quality controlled
- Labels in three modalities
 - Sentinel-1 weak labels (Otsu threshold in the VV-band)
 - **Sentinel-2 weak labels** (NDVI and MNDWI ratios)
 - **Hand-labels**

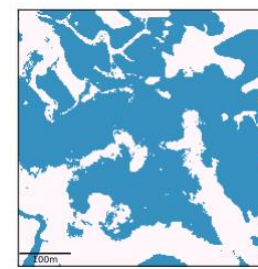
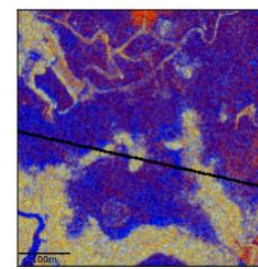
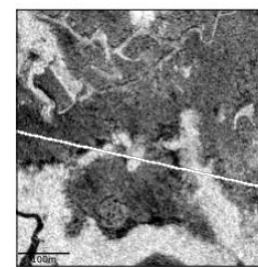
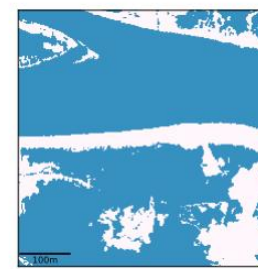
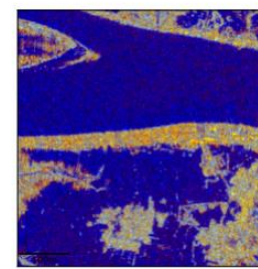
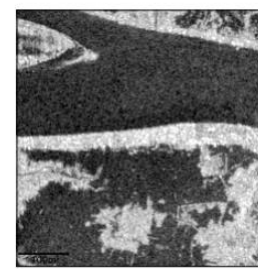
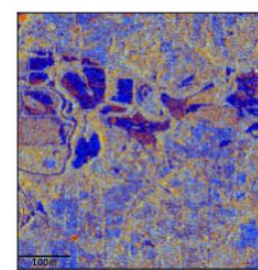
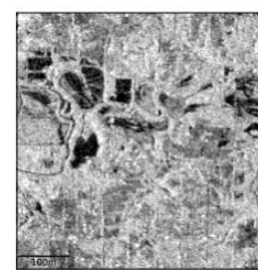
SEN1FLOODS11 DATA SET

- This study uses a subset of the Sen1Floods11 data set
- **Geographically diverse:** USA, Mekong, Bolivia, India, Paraguay, Colombia, and Sri-Lanka
- Sen1Floods11 data set provides the co-event intensity data
- **Sri-Lanka** kept as a generalization data set



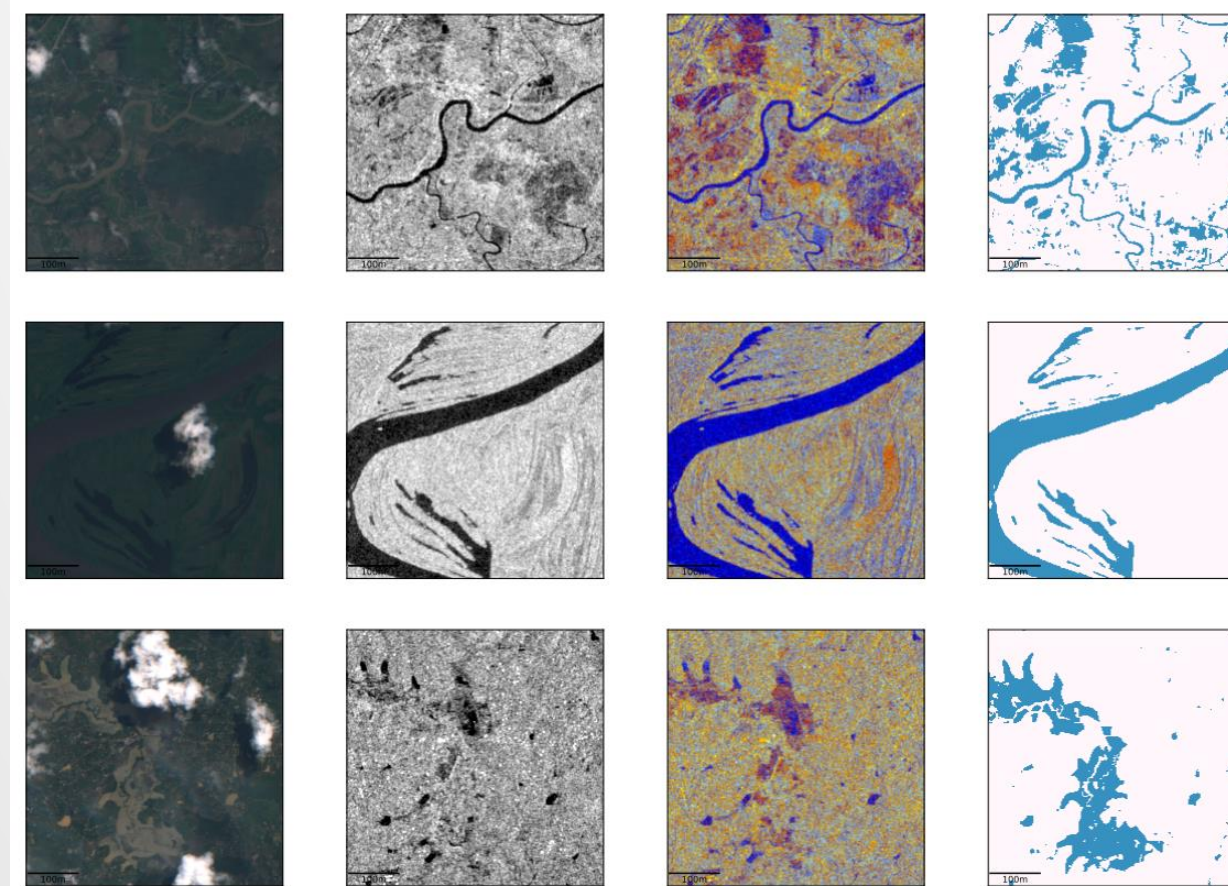
Geographical regions from where flood data was sampled. Adapted from [13]

SEN1FLOODS11 DATA SET - EXAMPLES



Sentinel-2 true color composite, Sentinel-1 (VV) intensity, Sentinel-1 false color composite (R: VV , G: VH, B: VV / VH), Hand-label [13]. Data processed with Python.

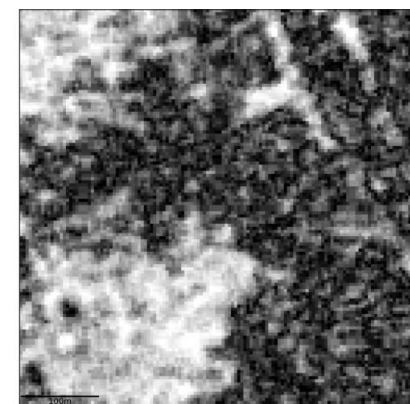
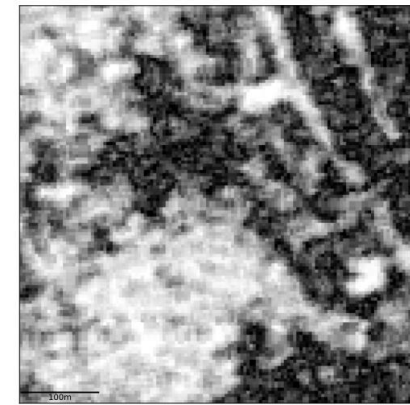
SEN1FLOODS11 DATA SET - EXAMPLES



Sentinel-2 true color composite, Sentinel-1 (VV) intensity, Sentinel-1 false color composite (R: VV , G: VH, B: VV / VH), Hand-label [13]. Data processed with Python.

DATA SET AUGMENTATION

- Pre-event ground range detected (GRD) chips downloaded from GEE [28]
 - GRD products processed to backscatter intensity (σ^0)
 - GRD products at 10-m resolution
- On-demand InSAR coherence from the Alaska Satellite Facility [10]



Pre-event intensity (VV) and coherence (top), co-event intensity (VV) and coherence (bottom). Sentinel-1 data processed by GEE [28], ASF [10] and Python.

INSAR PRODUCTS

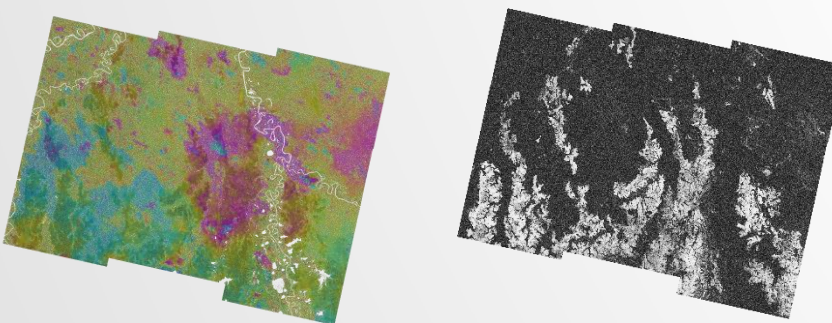
- Interferometry requires a pair of co-registered single-look complex (SLC) Sentinel-1 acquisitions
- The temporal and perpendicular baselines affect how correlated the scenes are

Country	Pre-event InSAR	Pre-event InSAR	Co-event InSAR	Co-event InSAR
	B_t (days)	B_p Range (m)	B_t (days)	B_p Range (m)
USA	12	5 - 6	12	21 - 22
KHM	12	114 - 117	12	37 - 38
BOL	12	24 - 29	12	4 - 6
IND	24	7 - 11	24	9 - 14
PRY	12	21 - 32	12	38 - 40
COL	12	46 - 50	12	0.2 - 1.1
LKA	12	76 - 80	6	71 - 80

Temporal and perpendicular baselines for InSAR products. Retrieved from ASF [10].

INSAR PROCESSING PIPELINE

- Final output is a geocoded interferogram and coherence map



Unwrapped phase interferogram (left) and coherence map (right) over Bolivia. Data retrieved from ASF [10].

Algorithm 2 InSAR Processing Pipeline [15]

Pre-Processing

- 1: Ingest SLC data into GAMMA format
- 2: Get DEM file covering the area, apply geoid correction and resample/reproject as required
- 3: Calculate overlapping bursts for input scenes
- 4: Mosaic swaths and bursts together

InSAR Processing

- 5: Prepare initial look-up table and simulated unwrapped image
 - Derive lookup table for SLC/MLI co-registration (considering terrain heights)
 - Simulate unwrapped interferometric phase using DEM height, and deformation rate using orbit state vectors
- 6: Interferogram creation, matching, refinement
 - Initial co-registration with look-up table
 - Iterative co-registration with look-up table
 - Removal of curved earth and topographic phase
- 7: Determine a co-registration offset based on the burst overlap (spectral diversity method)
 - Single iteration co-registration with look-up table
- 8: Phase unwrapping and coherence map generation
- 9: Generation of displacement maps from unwrapped differential phase

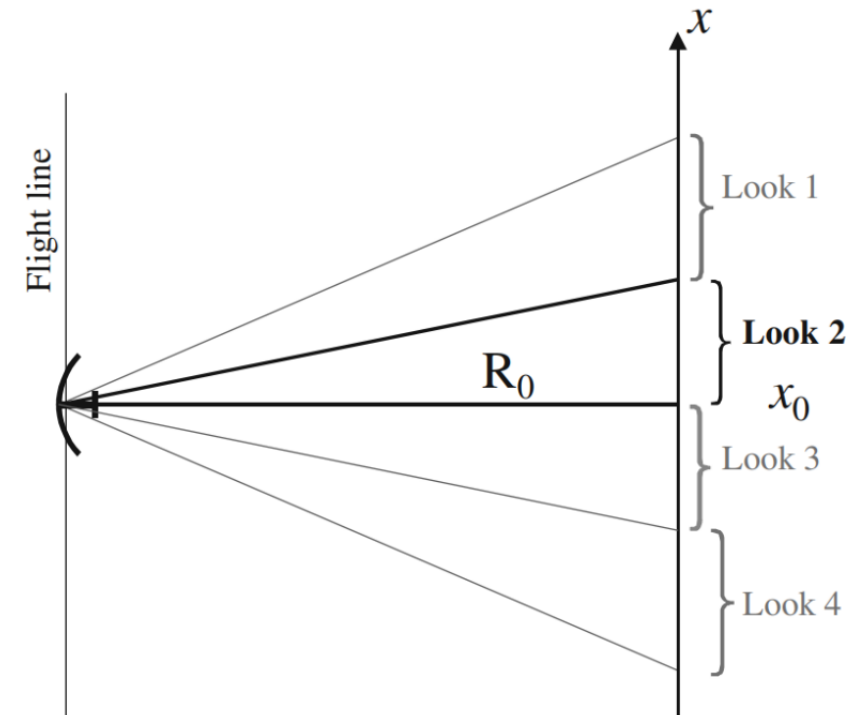
Post-Processing

- 10: Generation of geocoded GeoTIFF outputs

InSAR processing pipeline. Retrieved from ASF [10].

A NOTE ON INSAR PRODUCTS

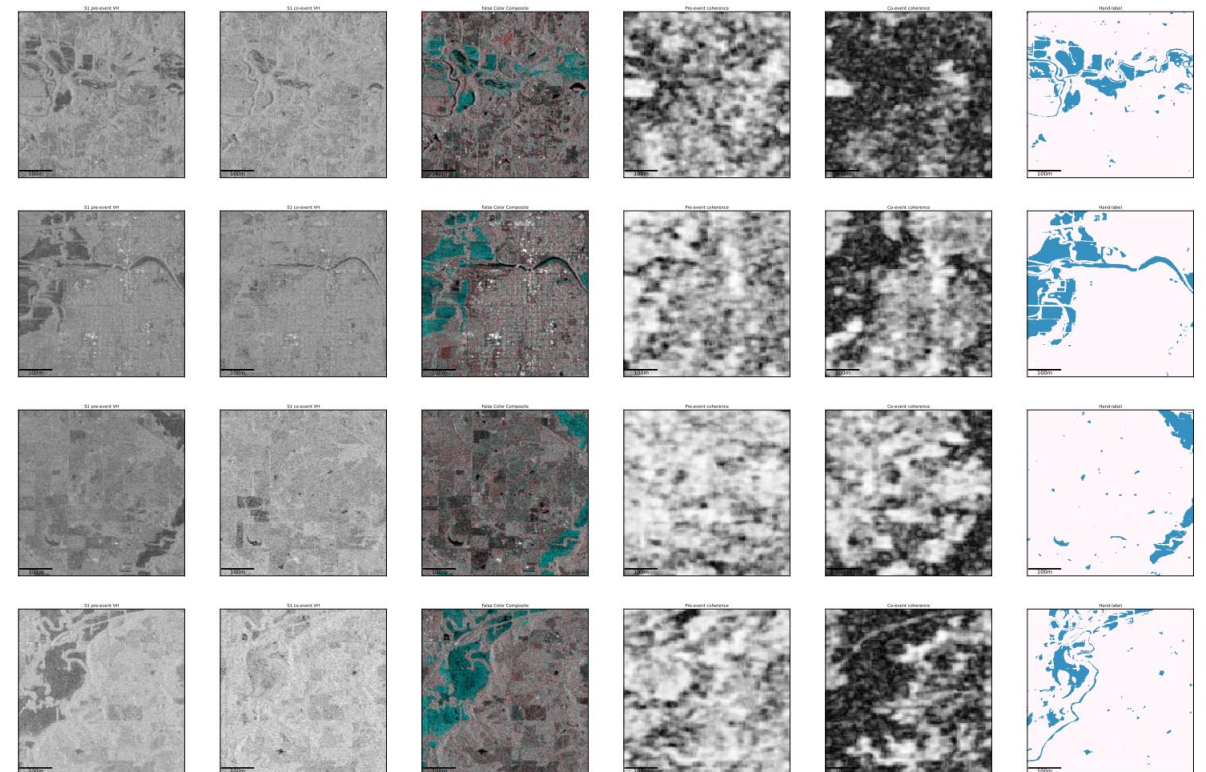
- ASF provides on-demand InSAR products at 40-m and 80-m resolution
 - Resolution is set by the number of multi-looks used in processing
- The on-demand products are generated using the GAMMA software and an HPC pipeline running on AWS
- **Coherence maps are resampled using GDAL and a nearest neighbor interpolation algorithm**
 - Non-linear resampling algorithms tend to smooth out the coherence map



SAR multi-look geometry. Adapted from [22]

COHERENCE MAPS

- Coherence maps range from uncorrelated (value of 0) to correlated (value of 1)
- During a flooding event, the co-event coherence drops relative to the pre-event coherence



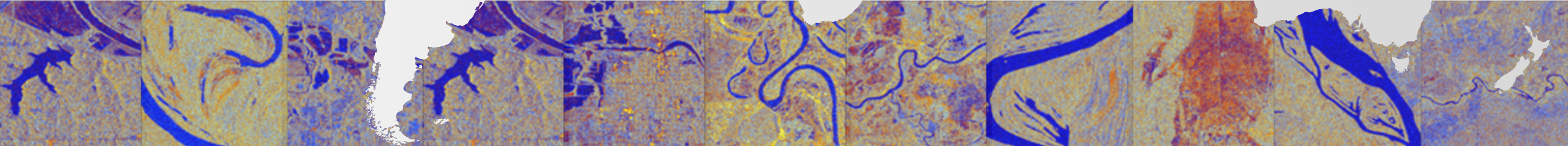
From left to right: co-event intensity (VH), pre-event intensity (VH), false color composite (R: co-event, G: pre-event, B: pre-event, adapted from [9]), pre-event coherence, co-event coherence, hand-label. Data retrieved from GEE [28], ASF [10], and post-processed with Python.

RECAP OF DATA AUGMENTATION

- Augment intensity with pre-event GRD products from Google Earth Engine [28]
- Augment data set with InSAR coherence from the Alaska Satellite Facility [10]
 - Resample from 40-m to 10-m



SEMANTIC WATER SEGMENTATION



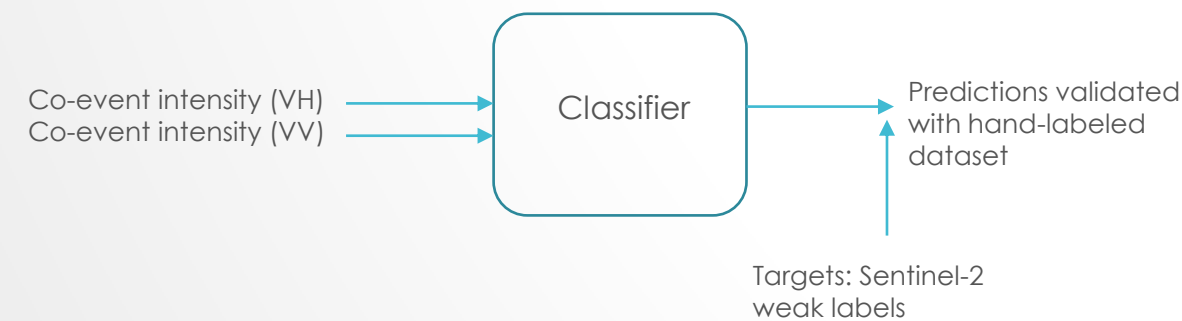
MODEL SCENARIOS

Scenario	Description	Number of channels
Scenario I	Co-event intensity	2
Scenario II	Pre-event intensity + Co-event Intensity	4
Scenario III	Pre-event intensity and coherence + Co-event intensity and coherence	6

Experimental scenarios. Inspired by [16]

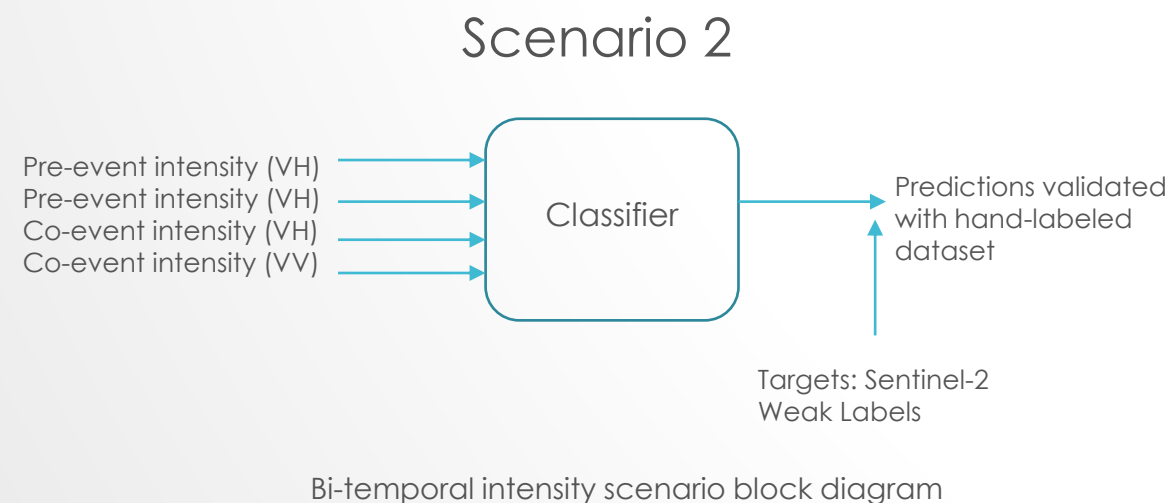
MODEL INPUTS AND LABELS USED BY SCENARIO

Scenario 1

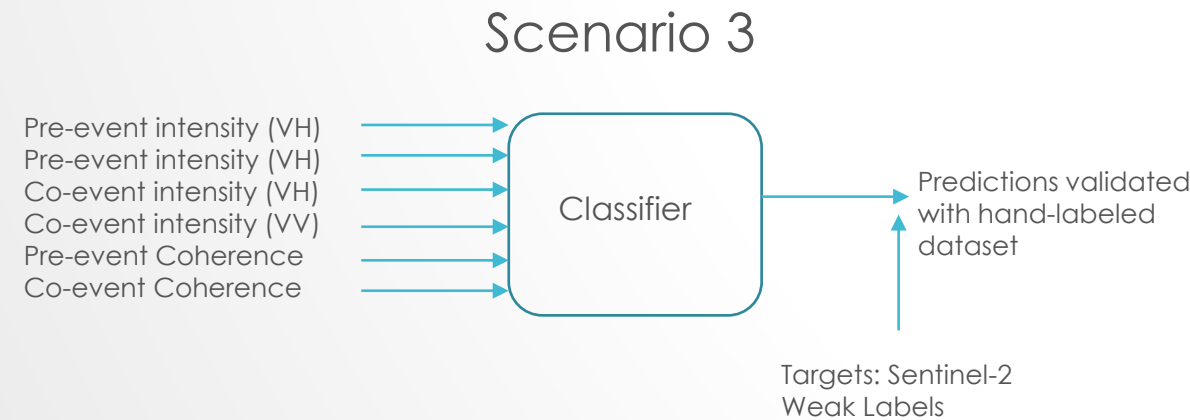


Uni-temporal intensity scenario block diagram

MODEL INPUTS AND LABELS USED BY SCENARIO



MODEL INPUTS AND LABELS USED BY SCENARIO

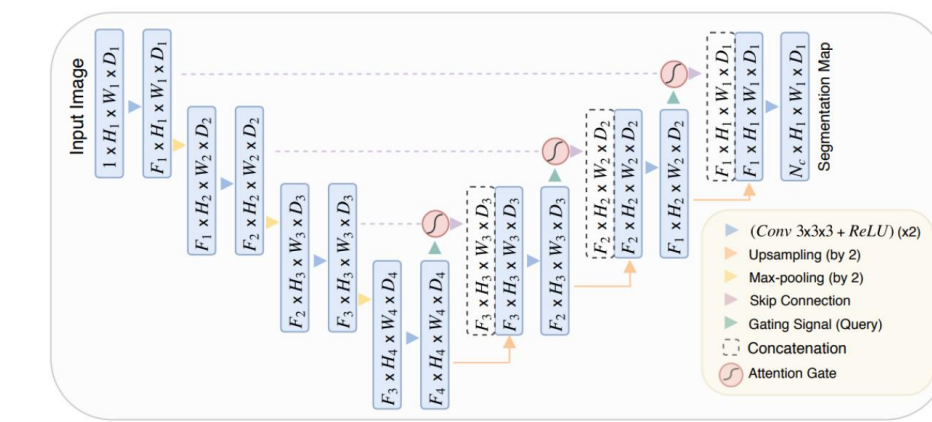


Bi-temporal intensity and coherence scenario block diagram

MACHINE LEARNING MODELS

- XGBoost
 - Classification tree ensemble algorithm
 - Pixel-wise classification
 - Input features are raw pixel values with no feature engineering
- Trained using Python's xgboost library [30]

- Attention U-Net
 - Encoder-decoder neural network architecture
 - Attention gates are introduced in the skip connection paths and learn to focus on the important spatial features of the input layers



Attention U-Net architecture. Adapted from [29]

MODEL TRAINING

- **XGBoost**
 - Binary segmentation with not-valid pixels mapped to not-water
 - Model with 100 estimators, learning rate of 0.3, and maximum tree depth of 6
 - Trained using NVIDIA RTX 3090 GPU in ~3 minutes
 - Model training was serialized to fit dataset into GPU memory (~28GB data set)

Region	Train Chips	Val Chips	Test Chips	Hand-labeled Chips
USA	300	68	76	60
Mekong	906	155	189	27
Colombia	362	60	77	0
Paraguay	212	38	40	61
India	315	55	59	63
Bolivia	121	16	19	10
Sri-Lanka	0	0	185	41
Totals	2216	392	645	262

Train, validation, and test data set splits

Data Set	Not-Water Pixels	Water Pixels	Not-Valid Pixels
S2 Weakly Labeled	82.14%	13.03%	4.83%
Hand-Labeled	82.87%	9.71%	7.42%

Pixel statistics distribution

MODEL TRAINING

- **Attention U-Net**
 - Binary segmentation with not-valid pixels mapped to not-water
 - Keras U-Net collection leveraged for the model [31]
 - VGG-16 backbone for decoder
 - Data augmentation: random 90-degree flips
 - Weights are trained from scratch to prevent negative learning
 - Trained using NVIDIA RTX 3090 GPU and Tensorflow in ~3 hours [32]

Region	Train Chips	Val Chips	Test Chips	Hand-labeled Chips
USA	300	68	76	60
Mekong	906	155	189	27
Colombia	362	60	77	0
Paraguay	212	38	40	61
India	315	55	59	63
Bolivia	121	16	19	10
Sri-Lanka	0	0	185	41
Totals	2216	392	645	262

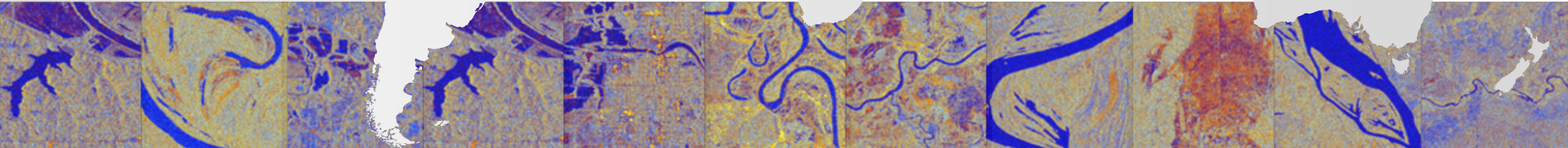
Train, validation, and test data set splits

Data Set	Not-Water Pixels	Water Pixels	Not-Valid Pixels
S2 Weakly Labeled	82.14%	13.03%	4.83%
Hand-Labeled	82.87%	9.71%	7.42%

Pixel statistics distribution



RESULTS



METRICS

- **Intersection over union**
 - Overlap between the predicted and ground truth labels divided by the union of the predicted and ground truth labels

$$IoU = \frac{TP}{TP + FP + FN}$$

- **Precision**
 - Ratio of correctly predicted positive observations to the total predicted positive observations. High precision relates to a low false positive rate

$$Precision = \frac{TP}{TP + FP}$$

METRICS

- **Recall**

- Ratio of correctly predicted positive observations to the total number of observations in the pertaining class. Recall answers the following question: **of all the water pixels, how many did we label as water?**

$$Recall = \frac{TP}{TP + FN}$$

- **F1-score**

- Weighted harmonic mean of precision and recall

$$F_1 = \frac{2 \times (precision \times recall)}{precision + recall}$$

CLASSIFICATION RESULTS

- We'll focus on the hand-labeled test data set results

A note on Sentinel-1 weak labels

- Models trained with Sentinel-1 weak labels overfit very quickly
- Experiments were also run with labels derived using HydroSAR and HYDRAFloods, and overfitting was observed

ATTENTION U-NET CLASSIFICATION RESULTS FOR ALL REGIONS

	Co-event Intensity	Pre- and co-event Int.	Pre- and co-event Int. and Coherence
Total mIoU	70.29%	67.70%	72.31%
Not Water IoU	86.01%	85.13%	86.76%
Water IoU	54.57%	50.27%	57.86%

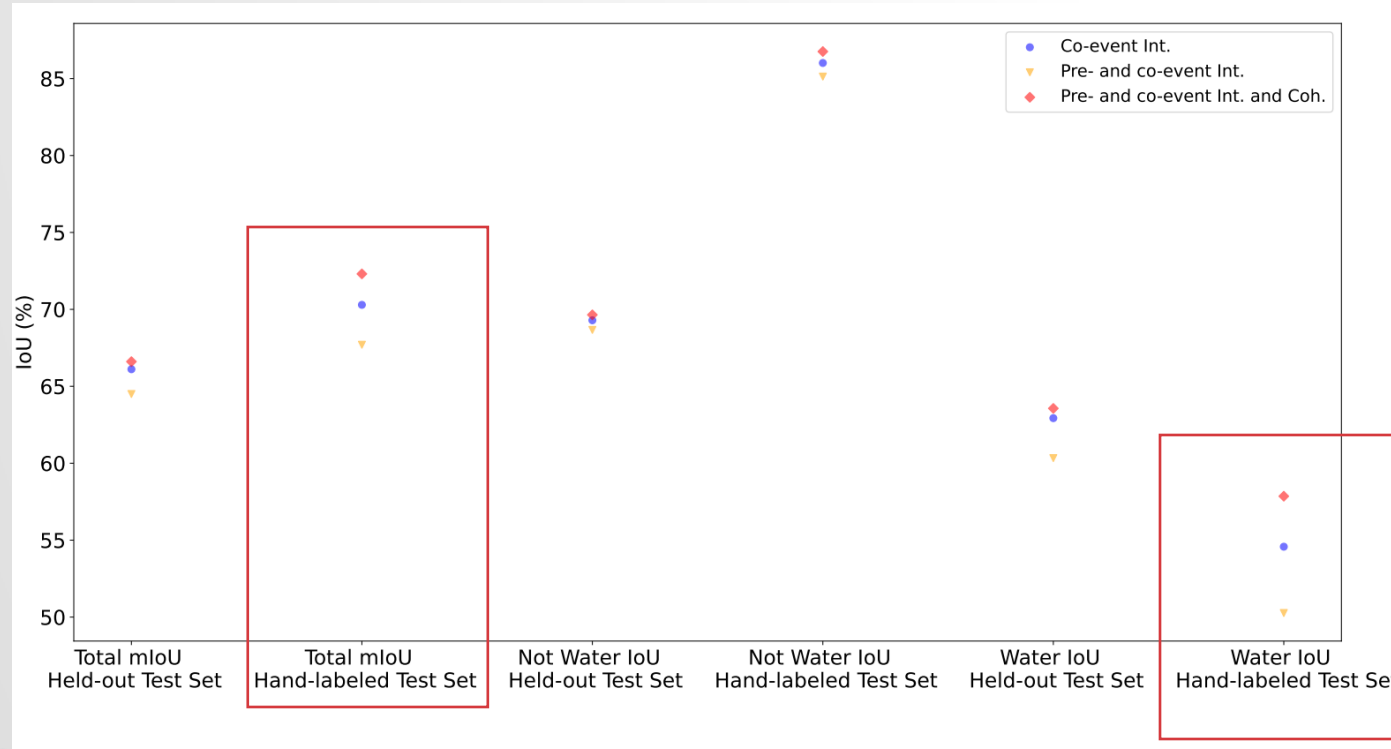
IoU Results for Attention U-Net Models,
Hand-Labeled Data Set

	Co-event Intensity	Pre- and co-event Int.	Pre- and co-event Int. and Coherence
Overall Accuracy	95.29%	94.94%	95.58%
Mean IoU	70.29%	67.70%	72.31%
Water Precision	86.63%	88.28%	85.90%
Water Recall	59.60%	53.86%	63.93%
Water f1-score	70.61%	66.90%	73.30%

Overall Results for Attention U-Net, Hand-Labeled Data Set

- Co-event intensity bands are the most relevant features for mapping surface water
 - Agrees with Sen1Floods11 findings and [16]
- Water IoU improves by **3.29%**
- Total mIoU improves by **2.02%**
- **Better recall implies the bi-temporal coherence data reduces the false negative rate | 4.33% improvement**
- **Water precision:** Bi-temporal intensity and coherence model **tends to over-estimate the water-class pixels** (i.e., higher false positive rate) | **-0.73%**
- **Some context:**
 - In [16] the authors use 1.2 m x 3.3 m TerraSAR-X data (X-band) and obtain 8 to 9% improvement for recall, precision, and f1-score for a single use case (Hurricane Harvey) and optimized model

ATTENTION U-NET IOU RESULTS FOR ALL REGIONS



IoU Results for Attention U-Net Models

- Water IoU improves by 3.29%
- Total mIoU improves by 2.02%

XGBOOST CLASSIFICATION RESULTS FOR ALL REGIONS

	Co-event Intensity	Pre- and co-event Int.	Pre- and co-event Int. and Coherence
Total mIoU	68.80%	69.30%	70.89%
Not Water IoU	85.23%	85.39%	85.92%
Water IoU	52.36%	53.20%	55.87%

IoU Results for XGBoost Models, Hand-Labeled Data Set

	Co-event Intensity	Pre- and co-event Int.	Pre- and co-event Int. and Coherence
Overall Accuracy	94.87%	94.93%	95.14%
Mean IoU	68.80%	69.30%	70.89%
Water Precision	80.15%	79.85%	79.06%
Water Recall	60.16%	61.45%	65.57%
Water f1-score	68.73%	69.45%	71.69%

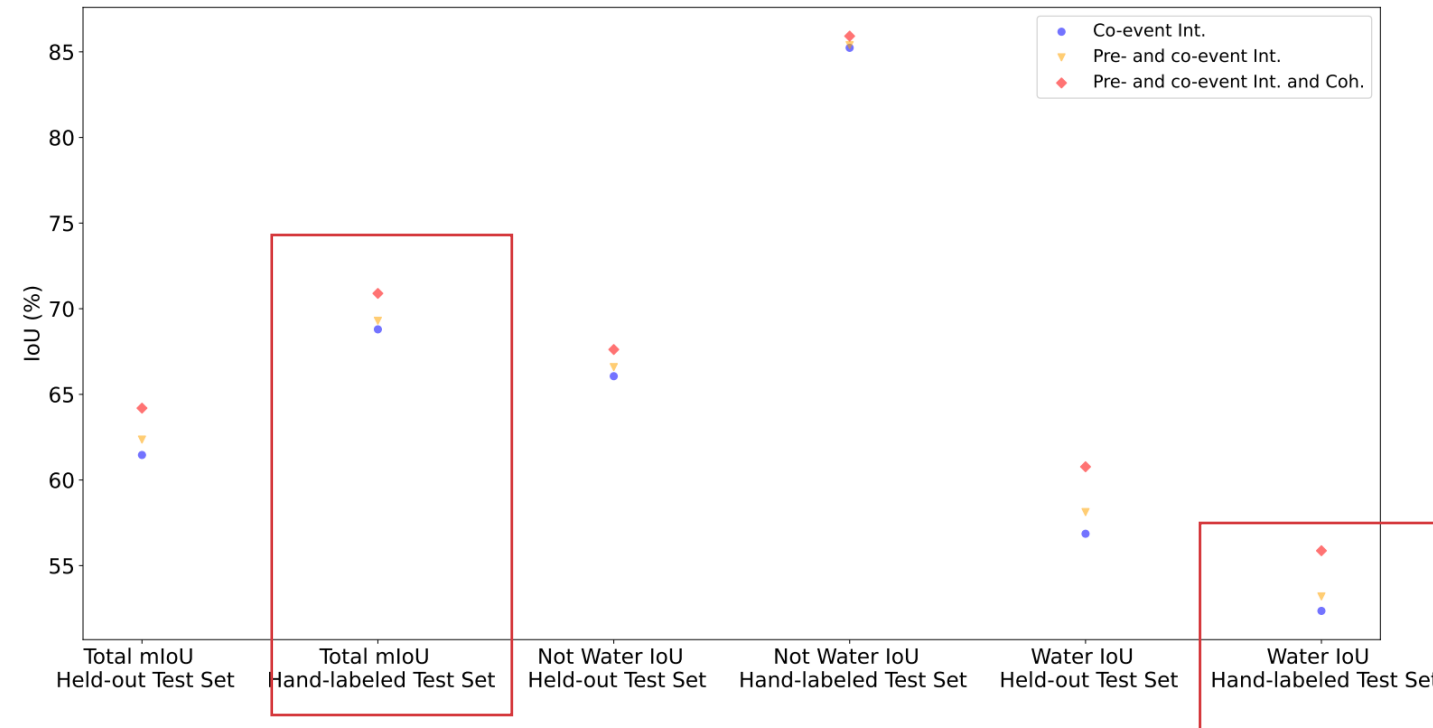
Overall Results for Attention U-Net, Hand-Labeled Data Set

- Water IoU improves by **3.51%**
- Total mIoU improves by **2.09%**
- **Water recall** improves by **5.33%**, reducing the false negative rate
- **Water Precision:** XGBoost model also tends to over-estimate water-class pixels (i.e., higher false positive rate) | **-1.09%**

- **Some context:**

- In [16] the authors use 1.2 m x 3.3 m TerraSAR-X data (X-band) and obtain 8 to 9% improvement for recall, precision, and f1-score for a single use case (Hurricane Harvey) and optimized model

XGBOOST IOU RESULTS FOR ALL REGIONS



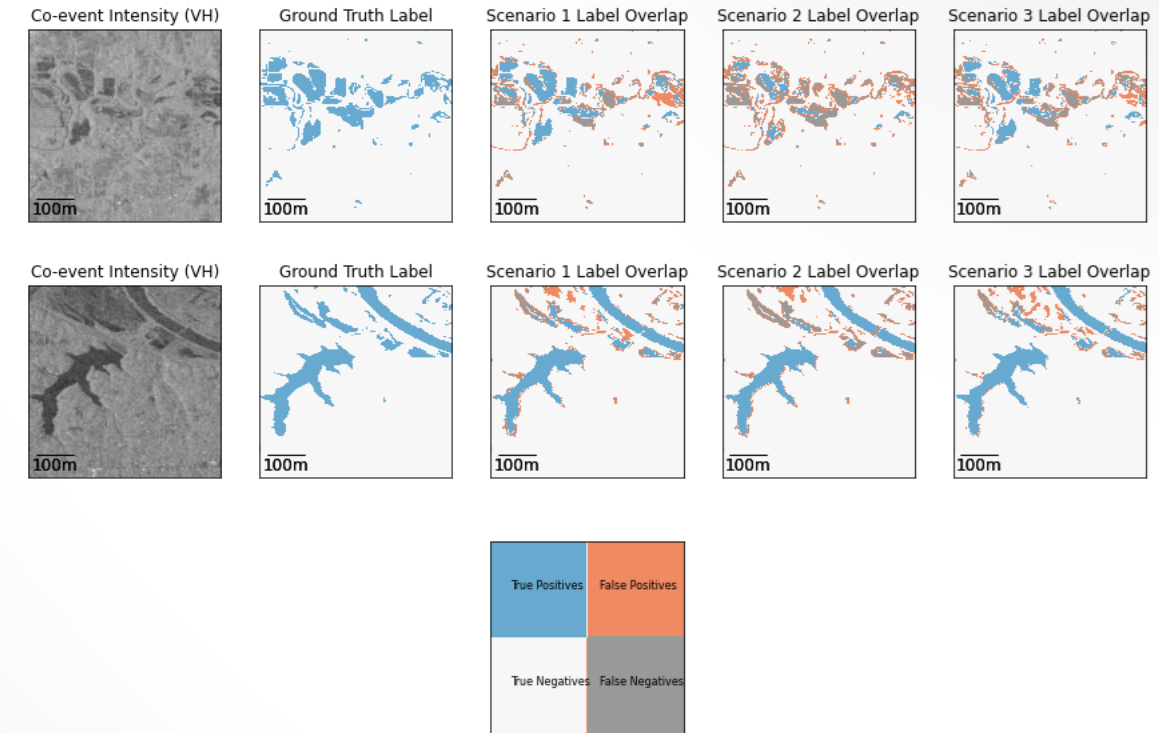
- Water IoU improves by 3.51%
- Total mIoU improves by 2.09% improvement

IoU Results for Attention U-Net Models

ATTENTION U-NET WATER IOU RESULTS BY REGION

- Scenario 3 outperforms scenarios 1 and 2 in terms of water IoU
- **Sri-Lanka (generalization data set) exhibits largest improvement**

	Co-event Int.	Pre- and co-event Int. and Coh.	Pre- and co-event Int.
USA	51.51%	51.43%	57.22%
Mekong	76.88%	67.13%	77.25%
Bolivia	09.61%	19.06%	37.96%
India	45.14%	40.52%	45.80%
Paraguay	54.13%	51.33%	58.19%
Sri-Lanka	1.09%	13.66%	39.49%



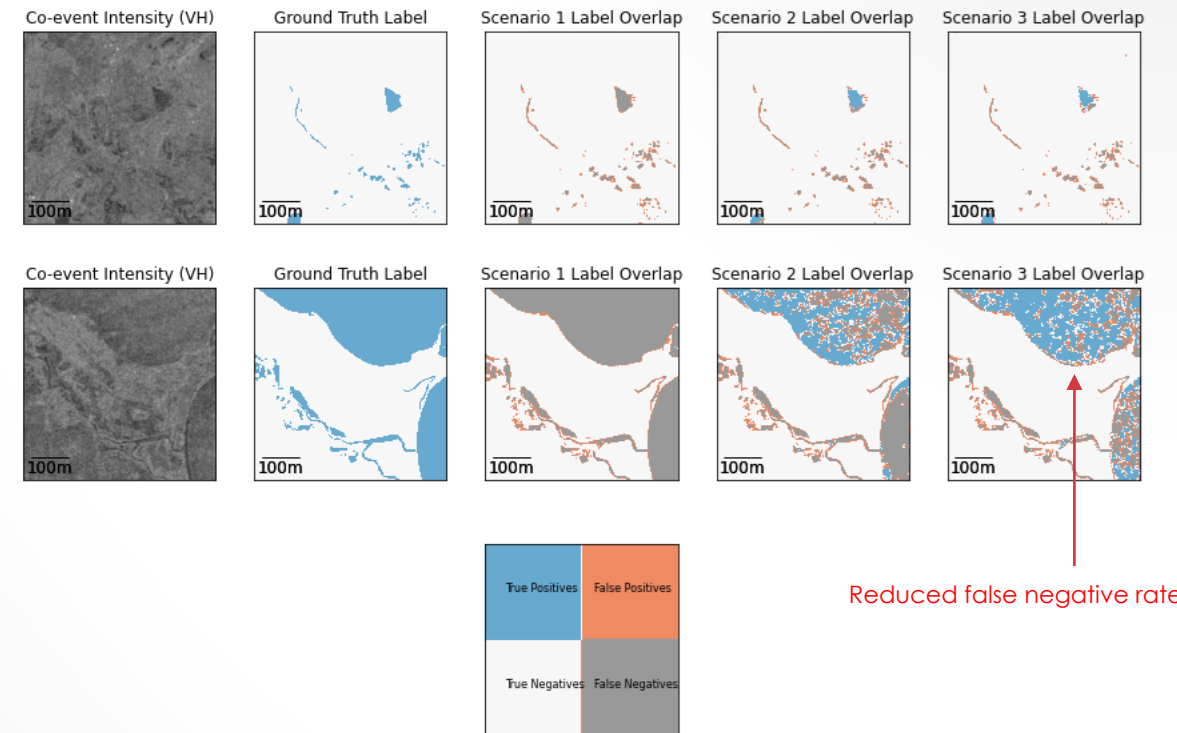
Label Overlay for USA, Attention U-Net

Regional Water IoU Results for Attention U-Net Models, Hand-Labeled Data Set

ATTENTION U-NET RECALL RESULTS BY REGION

- Scenario 3 outperforms scenarios 1 and 3 in terms of water recall
- **Scenario 3 reduces false negative rate**

	Co-event Intensity	Pre- and co-event Int. and Coherence	Pre- and co-event Int.
Bolivia	9.95%	20.51%	45.78%
India	50.29%	44.00%	51.72%
Mekong	84.18%	72.48%	84.46%
Paraguay	56.21%	52.79%	60.95%
USA	58.86%	55.84%	63.83%
Sri-Lanka	1.09%	13.69%	40.41%



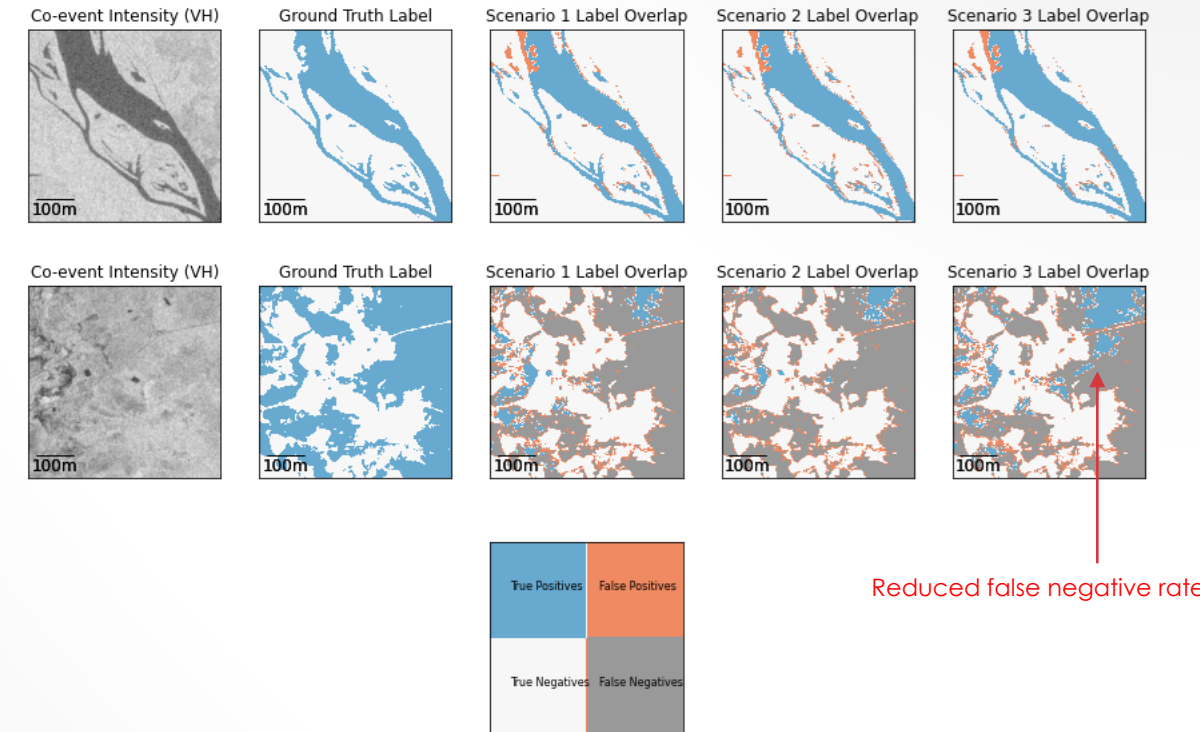
Label Overlay for Sri-Lanka, Attention U-Net

Regional Recall Results for Attention U-Net Models, Hand-Labeled Data Set

ATTENTION U-NET F1-SCORE RESULTS BY REGION

- Scenario 3 outperforms scenarios 1 and 3 in terms of water f1-score

	Co-event Intensity	Pre- and co-event Int. and Coherence	Pre- and co-event Int.
Bolivia	17.54%	32.02%	55.03%
India	62.20%	57.67%	62.83%
Mekong	86.93%	80.33%	87.16%
Paraguay	70.24%	67.84%	73.57%
USA	68.00%	67.93%	72.79%
Sri-Lanka	2.16%	24.03%	56.62%



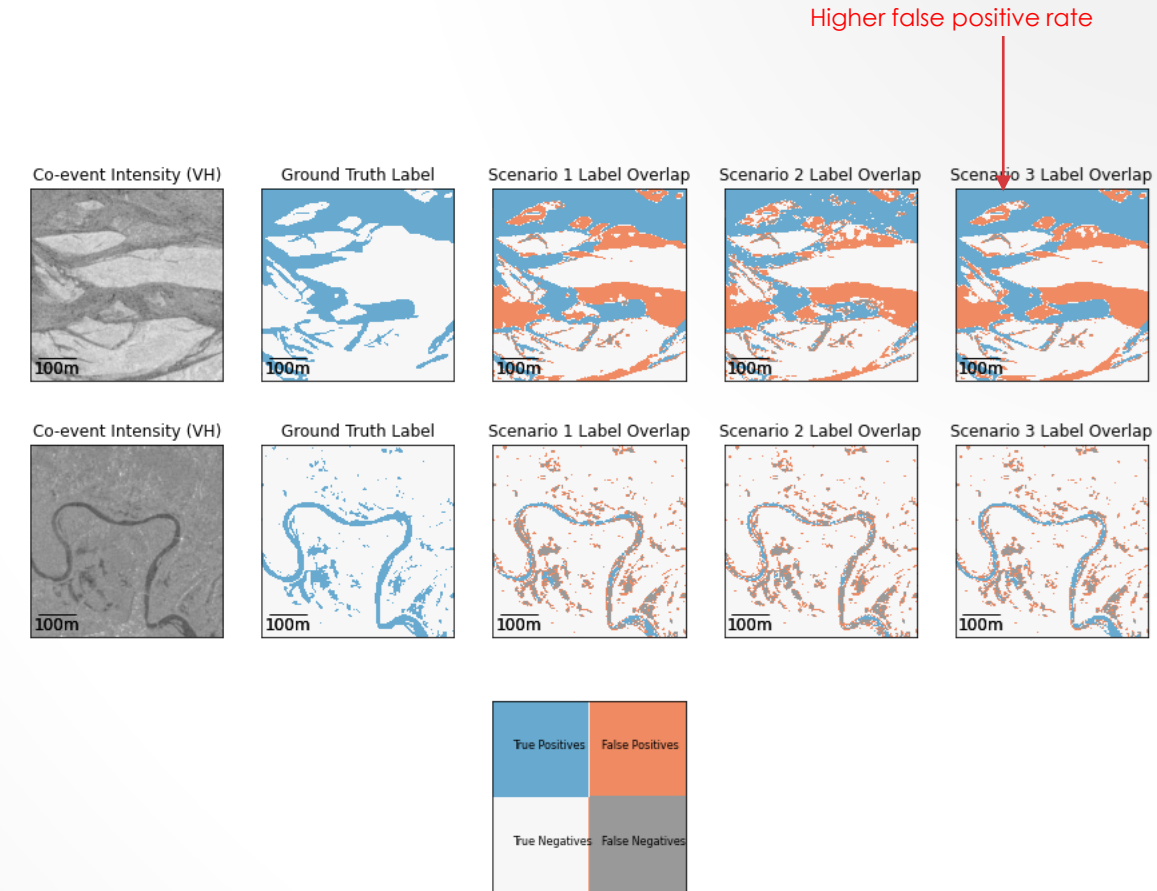
Label Overlay for Paraguay, Attention U-Net

Regional F1-Score Results for Attention U-Net Models, Hand-Labeled Data Set

ATTENTION U-NET PRECISION RESULTS BY REGION

- Scenario 2 outperforms scenarios 1 and 3 in terms of water precision
- **Scenario 3 over-estimates water pixels**

	Co-event Intensity	Pre- and co-event Int. and Coherence	Pre- and co-event Int.
Bolivia	73.82%	72.92%	68.94%
India	81.49%	83.66%	80.00%
Mekong	89.87%	90.09%	90.04%
Paraguay	93.60%	94.88%	92.78%
USA	80.49%	86.69%	84.66%
Sri-Lanka	85.51%	98.49%	94.56%



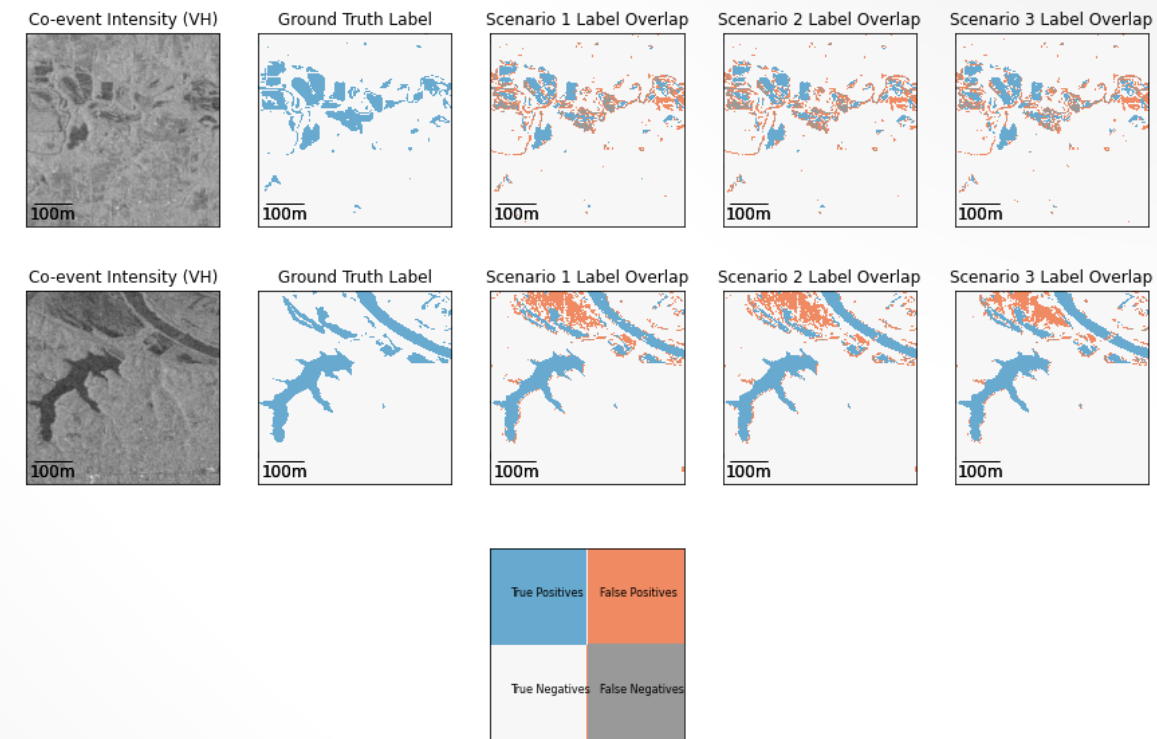
Label Overlap for India, Attention U-Net

Regional Precision Results for Attention U-Net Models,
Hand-Labeled Data Set

XGBOOST IOU RESULTS BY REGION

- Scenario 3 outperforms scenarios 1 and 2 in terms of water IoU
- **Sri-Lanka (generalization data set) exhibits largest improvement**

	Co-event Int.	Pre- and co-event Int.	Pre- and co-event Int. and Coh.
USA	49.32%	52.87%	55.06%
Mekong	68.85%	69.16%	72.95%
Bolivia	30.30%	30.89%	37.45%
India	44.53%	46.13%	47.74%
Paraguay	49.61%	48.35%	51.78%
Sri-Lanka	22.72%	33.54%	48.94%



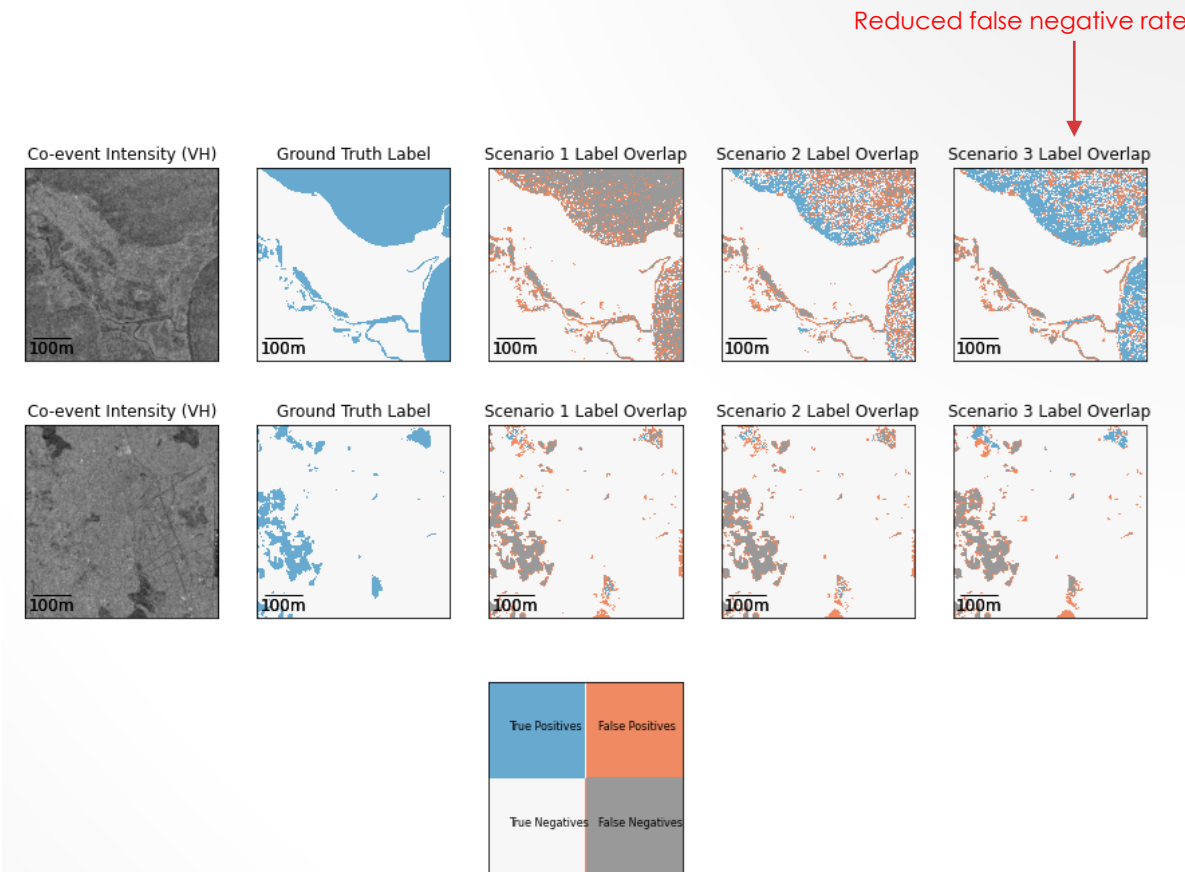
Label Overlap for USA, XGBoost

Regional IoU Results for XGBoost Models,
Hand-Labeled Data Set

XGBOOST RECALL RESULTS BY REGION

- Scenario 3 outperforms scenarios 1 and 3 in terms of water recall
- **Scenario 3 reduces false negative rate**

	Co-event Intensity	Pre- and co-event Int. and Coherence	Pre- and co-event Int.
Bolivia	42.95%	43.84%	60.29%
India	50.56%	53.56%	57.90%
Mekong	74.39%	74.89%	79.52%
Paraguay	55.59%	55.50%	60.44%
USA	64.66%	65.82%	64.34%
Sri-Lanka	23.82%	34.97%	51.64%



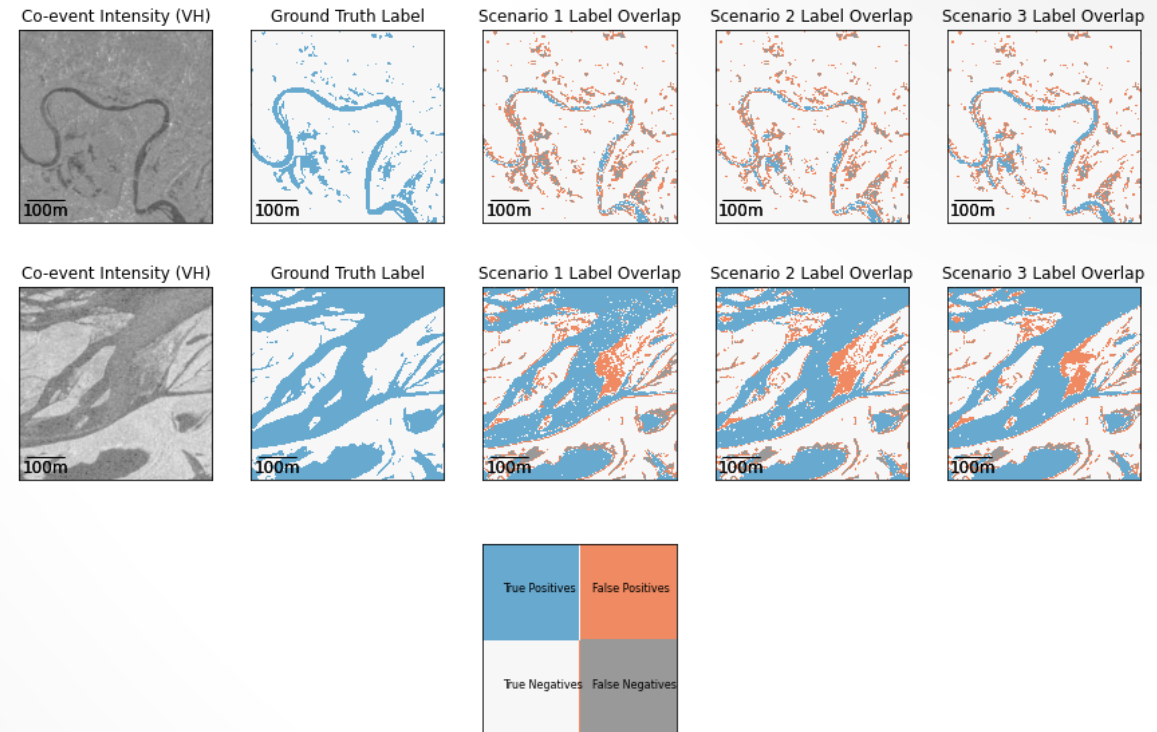
Label Overlap for Sri-Lanka, XGBoost

Regional Recall Results for XGBoost Models, Hand-Labeled Data Set

XGBOOST F1-SCORE RESULTS BY REGION

- Scenario 3 outperforms scenarios 1 and 3 in terms of water f1-score

	Co-event Intensity	Pre- and co-event Int. and Coherence	Pre- and co-event Int.
Bolivia	46.51%	47.20%	54.50%
India	61.62%	63.13%	64.63%
Mekong	81.55%	81.77%	84.36%
Paraguay	66.32%	65.18%	68.23%
USA	66.06%	69.17%	71.02%
Sri-Lanka	37.03%	50.24%	65.72%



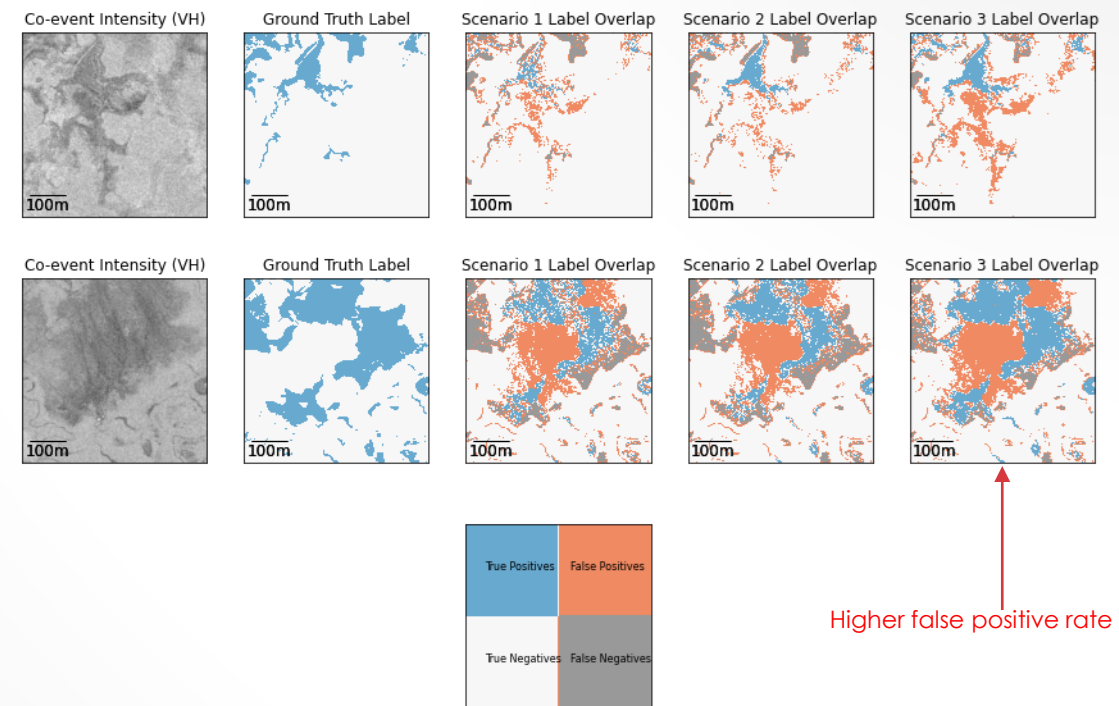
Label Overlap for India, XGBoost

Regional F1-Score Results for XGBoost Models, Hand-Labeled Data Set

XGBOOST PRECISION RESULTS BY REGION

- Water precision results are more mixed for XGBoost models
- Scenario 3 over-estimates water pixels**

	Co-event Intensity	Pre- and co-event Int. and Coherence	Pre- and co-event Int.
Bolivia	50.71%	51.13%	49.72%
India	78.89%	76.88%	73.12%
Mekong	90.24%	90.03%	89.82%
Paraguay	82.18%	78.97%	78.33%
USA	67.52%	72.89%	79.25%
Sri-Lanka	83.17%	89.16%	90.35%



Label Overlap for Bolivia, XGBoost

Regional Precision Results for XGBoost Models, Hand-Labeled Data Set

CONCLUSIONS

- Sentinel-1 (10-m) backscatter intensity and InSAR coherence were fused in uni- and bi-temporal classification models
- Models cross-trained using Sentinel-2 water masks
- Pixel-wise XGBoost classifiers and CNN-based Attention U-Net classifiers were trained
- Sen1Floods11 data set used as the backbone and augmented with:
 - **Temporal augmentation:** pre-event intensity using Google Earth Engine [28]
 - **InSAR augmentation:** pre- and co-event InSAR coherence using ASF [10]

CONCLUSIONS

- Bi-temporal intensity and coherence fusion models improve IoU by:
 - Attention U-Net: **3.29%**
 - XGBoost: **3.51%**
- Both Attention U-Net and XGBoost models systematically reduce false negatives rate. Models improve water recall by:
 - Attention U-Net: **4.33%**
 - XGBoost: **5.41%**
- Bi-temporal intensity and coherence fusion models tend to underperform in terms of false positive rate. Water precision:
 - Attention U-Net: **-1.09%**
 - XGBoost: **-0.73%**
- Implication: freely available on-demand InSAR products from ASF can be used to improve semantic water segmentation

POTENTIAL FUTURE WORK

- Model tuning
 - Hyperparameter search
 - Feature engineering for XGBoost models
- **Augment data set to include urban flood events**
- Coherence to NDVI correlation / analysis
- Conditional Models



ACKNOWLEDGMENT

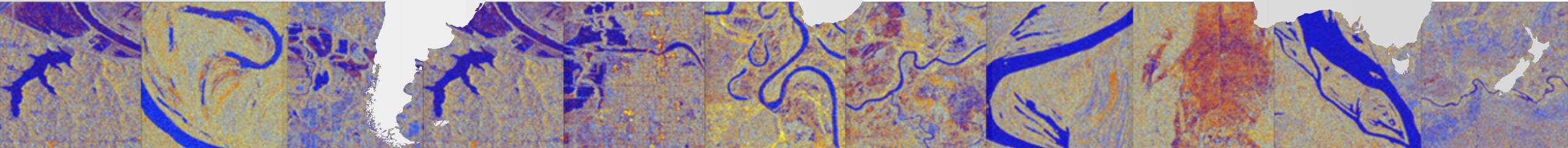


- I would like to thank the following individuals: Sam Keene, Krishna Karra, Chris Curro and all my Cooper Union professors
- Beth Tellman, Rohit Mukherjee, Hannah Friedrich, and the extended THP team
- I would like to thank Batu Osmanoglu, MinJeong Jo, Elodie Macorps, and Rustem Albayrak from NASA GSFC
- I would also like to thank my family, Jade Da Silva Lima, Yuval Ofek and all my friends, and colleagues for their support and encouragement.





Q&A



REFERENCES

- [1] ESA, "Satellites support latest IPCC Climate Report," february 2022. [Online]. Available: https://www.esa.int/Applications/Observing_the_Earth/_Space_for_our_climate/Satellites_support_latest_IPCC_climate_report
- [2] H.-O. Pörtner, D. Roberts, E. Poloczanska, K. Mintenbeck, M. Tignor, A. Alegría, M. Craig, S. Langsdorf, S. L'oschke, V. Möller, and A. Okem, "IPCC, 2022: Summary for Policymakers," 2022. [Online]. Available: https://report.ipcc.ch/ar6wg2/pdf/IPCC_AR6_WGII_SummaryForPolicymakers.pdf
- [3] "1.47 billion people face flood risk worldwide: For over a third, it could be devastating," Accessed: 2022-03-01. [Online]. Available: <https://blogs.worldbank.org/climatechange/147-billion-people-face-flood-risk-worldwide-over-third-it-could-be-devastating>
- [4] J. Rentschler and M. Salhab, "People in harm's way," Oct 2020, Accessed: 2022-03-01. [Online]. Available: <https://openknowledge.worldbank.org/handle/10986/34655?show=full>
- [5] N. Otsu, "A threshold selection method from gray-level histograms," IEEE Trans. Sys. Man. Cyber. 9 (1), pp. 62–66, 1979.
- [6] R. Gonzalez and R. E. Woods, Digital Image Processing, 4th Ed. New York, NY: Pearson, 2018.
- [7] Hydrosar training: Extracting flood information from SAR," Accessed: Fall 2021. [Online]. Available: <https://servir.icimod.org/events/hydrosar-training-extracting-flood-information-from-sar/>
- [8] F. Meyer, "Hydrosar project. Github repository."
- [9] A. Twele, W. Cao, S. Plank, and S. Martinis, "Sentinel-1-based flood mapping: a fully automated processing chain," International Journal of Remote Sensing, vol. 37, pp. 2990 – 3004, 2016.
- [10] ASF, "Alaska satellite facility, UAF," Accessed: Fall 2021, Spring 2022. [Online]. Available: <https://ASF.alaska.edu>
- [11] HYDRAFloods, "Hydrafloods documentation." [Online]. Available: <https://servir-mekong.github.io/hydra-floods/algorithms/>

REFERENCES

- [12] V. Katiyar, N. Tamkuan, and M. Nagai, "Near-real-time flood mapping using off-the-shelf models with sar imagery and deep learning," *Remote Sensing*, vol. 13, no. 12, 2021. [Online]. Available: <https://www.mdpi.com/2072-4292/13/12/2334>
- [13] D. Bonafilia, B. Tellman, T. Anderson, and E. Issenberg, "Sen1floods11: a georeferenced dataset to train and test deep learning flood algorithms for sentinel-1," 2020 IEEE/CVF Conference on Computer Vision and Pattern Recognition Workshops (CVPRW), pp. 835–845, 2020.
- [14] B. Peng, Q. Huang, J. Vongkusolkit, S. Gao, D. B. Wright, Z. N. Fang, and Y. Qiang, "Urban flood mapping with bitemporal multispectral imagery via a self-supervised learning framework," *IEEE Journal of Selected Topics in Applied Earth Observations and Remote Sensing*, vol. 14, pp. 2001–2016, 2021.
- [15] T. Mayer, A. Poortinga, B. Bhandari, A. P. Nicolau, K. Markert, N. S. Thwal, A. Markert, A. Haag, J. Kilbride, F. Chishtie, A. Wadhwa, N. Clinton, and D. Sagha, "Deep learning approach for sentinel-1 surface water mapping leveraging google earth engine," *ISPRS Open Journal of Photogrammetry and Remote Sensing*, vol. 2, 2021.
- [16] Y. Li, S. Martinis, and M. Wieland, "Urban flood mapping with an active self-learning convolutional neural network based on terrasar-x intensity and interferometric coherence," *ISPRS Journal of Photogrammetry and Remote Sensing*, 2019
- [17] L. Pulvirenti, M. Chini, N. Pierdicca, and G. Boni, "Use of sar data for detecting floodwater in urban and agricultural areas: The role of the interferometric coherence," *IEEE Transactions on Geoscience and Remote Sensing*, vol. 54, pp. 1532–1544, 2016.
- [18] M. Chini, R. Pelich, L. Pulvirenti, N. Pierdicca, R. Hostache, and P. Matgen, "Sentinel-1 InSAR coherence to detect floodwater in urban areas: Houston and hurricane harvey as a test case," *Remote. Sens.*, vol. 11, p. 107, 2019.
- [19] C. Chaabani, M. Chini, R. Abdelfattah, R. Hostache, and K. Chokmani, "Flood mapping in a complex environment using bistatic tandem-x/terrasar-x insar coherence," *Remote. Sens.*, vol. 10, p. 1873, 2018.
- [20] F. Meyer, "Synthetic Aperture Radar: Hazards [MOOC]," 2021, Accessed: Fall, 2021. [Online]. Available: <https://www.edx.org/course/sar-hazards>
- [21] A. Flores, K. Herndon, R. Thapa, and E. Cherrington, *The SAR Handbook: Comprehensive Methodologies for Forest Monitoring and Biomass Estimation*, 2019.

REFERENCES

- [22] I. Woodhouse, Introduction to Microwave Remote Sensing, 1st Ed. CRC Press, 2006.
- [23] E. Podest, S. McCartney, E. Fielding, A. L. Handwerger, and N. A. G. Brook, "SAR for Disasters and Hydrological Applications," 2019. [Online]. Available: <https://appliedsciences.nasa.gov/join-mission/training/english/arset-sar-disasters-and-hydrological-applications>
- [24] E. Podest, N. Pinto, and E. Fielding, "Introduction to Synthetic Aperture Radar," 2017. [Online]. Available: <https://appliedsciences.nasa.gov/join-mission/training/english/arset-introduction-synthetic-aperture-radar>
- [25] ESA, "Sentinel-1 - Missions." [Online]. Available: <https://sentinel.esa.int/web/sentinel/missions/sentinel-1>
- [26] ESA, "Sentinel-1 - Data Products," Accessed: February 2022. [Online]. Available: <https://sentinel.esa.int/web/sentinel/missions/sentinel-1/data-products>
- [27] "Cloud to Street." [Online]. Available: <https://www.cloudtostreet.ai/>
- [28] N. Gorelick, M. Hancher, M. Dixon, S. Ilyushchenko, D. Thau, and R. Moore, "Google Earth Engine: Planetary-scale geospatial analysis for everyone," 2017. [Online]. Available: <https://doi.org/10.1016/j.rse.2017.06.031>
- [29] O. Oktay, J. Schlemper, L. L. Folgoc, M. J. Lee, M. P. Heinrich, K. Misawa, K. Mori, S. G. McDonagh, N. Y. Hammerla, B. Kainz, B. Glocker, and D. Rueckert, "Attention U-Net: Learning Where to Look for the Pancreas," ArXiv, vol. abs/1804.03999, 2018.
- [30] T. Chen and C. Guestrin, "XGBoost: A Scalable Tree Boosting System," Proceedings of the 22nd ACM SIGKDD International Conference on Knowledge Discovery and Data Mining, 2016.
- [31] Y. Sha, "Keras-unet-collection. GitHub repository," 2021. [Online]. Available: <https://github.com/yingkaisha/keras-unet-collection>

REFERENCES

- [32] M. Abadi, A. Agarwal, P. Barham, E. Brevdo, Z. Chen, C. Citro, G. S. Corrado, A. Davis, J. Dean, M. Devin, S. Ghemawat, I. Goodfellow, A. Harp, G. Irving, M. Isard, Y. Jia, R. Jozefowicz, L. Kaiser, M. Kudlur, J. Levenberg, D. Man  e, R. Monga, S. Moore, D. Murray, C. Olah, M. Schuster, J. Shlens, B. Steiner, I. Sutskever, K. Talwar, P. Tucker, V. Vanhoucke, V. Vasudevan, F. Vi  gas, O. Vinyals, P. Warden, M. Wattenberg, M. Wicke, Y. Yu, and X. Zheng, "TensorFlow: 170 Large-Scale Machine Learning on Heterogeneous Systems," 2015, software available from tensorflow.org. [Online]. Available: <http://tensorflow.org/> [23] E. Podest, S. McCartney, E. Fielding, A. L. Handwerger, and N. A. G. Brook, "SAR for Disasters and Hydrological Applications," 2019. [Online]. Available: <https://appliedsciences.nasa.gov/join-mission/training/english/arset-sar-disasters-and-hydrological-applications>
- [24] E. Podest, N. Pinto, and E. Fielding, "Introduction to Synthetic Aperture Radar," 2017. [Online]. Available: <https://appliedsciences.nasa.gov/join-mission/training/english/arset-introduction-synthetic-aperture-radar>
- [25] ESA, "Sentinel-1 - Missions." [Online]. Available: <https://sentinel.esa.int/web/sentinel/missions/sentinel-1>
- [26] ESA, "Sentinel-1 - Data Products," Accessed: February 2022. [Online]. Available: <https://sentinel.esa.int/web/sentinel/missions/sentinel-1/data-products>
- [27] "Cloud to Street." [Online]. Available: <https://www.cloudtostreet.ai/>
- [28] N. Gorelick, M. Hancher, M. Dixon, S. Ilyushchenko, D. Thau, and R. Moore, "Google Earth Engine: Planetary-scale geospatial analysis for everyone," 2017. [Online]. Available: <https://doi.org/10.1016/j.rse.2017.06.031>
- [29] O. Oktay, J. Schlemper, L. L. Folgoc, M. J. Lee, M. P. Heinrich, K. Misawa, K. Mori, S. G. McDonagh, N. Y. Hammerla, B. Kainz, B. Glocker, and D. Rueckert, "Attention U-Net: Learning Where to Look for the Pancreas," ArXiv, vol. abs/1804.03999, 2018.
- [30] T. Chen and C. Guestrin, "XGBoost: A Scalable Tree Boosting System," Proceedings of the 22nd ACM SIGKDD International Conference on Knowledge Discovery and Data Mining, 2016.
- [31] Y. Sha, "Keras-unet-collection. GitHub repository," 2021. [Online]. Available: <https://github.com/yingkaisha/keras-unet-collection>



BACKUP SLIDES



THECOOPERUNION

ATTENTION U-NET VERSUS XGBOOST ALL REGIONS

	Attention U-Net Scenario 1	XGBoost Scenario 1
Overall Accuracy	95.29%	94.87%
Mean IoU	70.29%	68.80%
Water Precision	86.63%	80.15%
Water Recall	59.60%	60.16%
Water f1-score	70.61%	68.73%

	Attention U-Net Scenario 2	XGBoost Scenario 2
Overall Accuracy	94.94%	94.93%
Mean IoU	67.70%	69.30%
Water Precision	88.28%	79.85%
Water Recall	53.86%	61.45%
Water f1-score	66.90%	69.45%

	Attention U-Net Scenario 3	XGBoost Scenario 3
Overall Accuracy	95.58%	95.14%
Mean IoU	72.31%	70.89%
Water Precision	85.90%	79.06%
Water Recall	63.93%	65.57%
Water f1-score	73.30%	71.69%

- Bi-temporal intensity and coherence model
 - **Mean IoU:** Attention U-Net outperforms XGBoost
 - **Recall:** XGBoost outperforms Attention U-Net.
 - XGBoost is better at reducing false negative rate
 - **Precision:** Attention U-Net wins.
 - Attention U-Net is better at reducing false positive rate
 - **F1-score:** Attention U-Net

ATTENTION U-NET VERSUS XGBOOST IOU RESULTS FOR ALL REGIONS

	Attention U-Net Scenario 1	XGBoost Scenario 1
Total mIoU	70.29%	68.80%
Not Water IoU	86.01%	85.23%
Water IoU	54.57%	52.36%

	Attention U-Net Scenario 2	XGBoost Scenario 2
Total mIoU	67.70%	69.30%
Not Water IoU	85.13%	85.39%
Water IoU	50.27%	53.20%

	Attention U-Net Scenario 3	XGBoost Scenario 3
Total mIoU	72.31%	70.89%
Not Water IoU	86.76%	85.92%
Water IoU	57.86%	55.87%

- Bi-temporal intensity and coherence model
 - Attention U-Net outperforms XGBoost model in terms of water IoU and mIoU

ATTENTION U-NET VERSUS XGBOOST GENERALIZATION DATA SET

	Attention U-Net Scenario 1	XGBoost Scenario 1
Water IoU	1.09%	22.72%
Water Recall	1.09%	23.82%
Water f1-score	2.16%	37.03%
Water Precision	85.51%	83.17%

	Attention U-Net Scenario 2	XGBoost Scenario 2
Water IoU	13.66%	33.54%
Water Recall	13.69%	34.97%
Water f1-score	24.03%	50.24%
Water Precision	98.49%	89.16%

	Attention U-Net - Scenario 3	XGBoost - Scenario 3
Water IoU	39.49%	48.94%
Water Recall	40.41%	51.64%
Water f1-score	56.62%	65.72%
Water Precision	94.56%	90.35%

- Bi-temporal intensity and coherence model
 - XGBoost is best at generalizing in terms of water IoU, recall, and f1-score
 - Attention U-Net is best at water precision



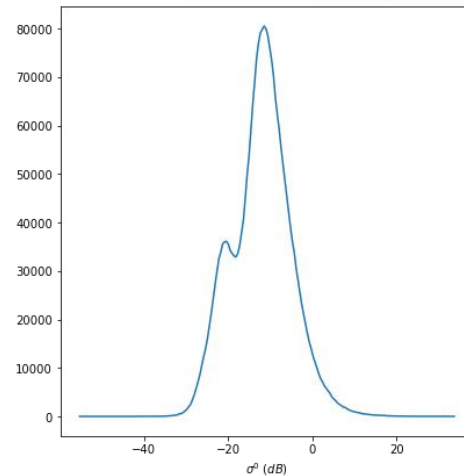
SURFACE WATER MAPPING WITH SAR BACKSCATTER INTENSITY



THE COOPER UNION

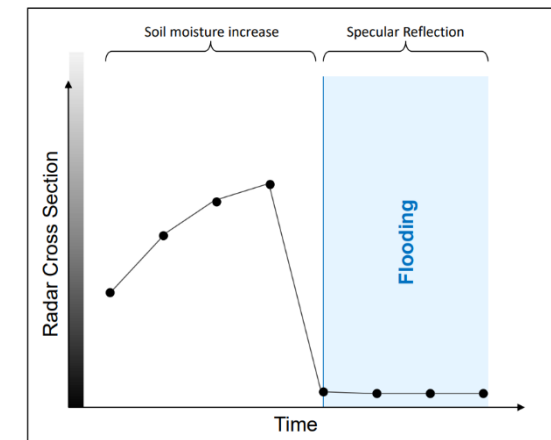
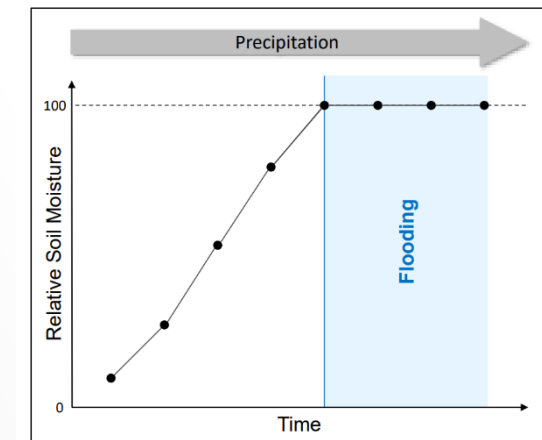
TYPICAL SAR INTENSITY DISTRIBUTION

- Pixel distribution is typically bi-modal
- Water bodies can be segmented using thresholding techniques (e.g., Otsu, K-means clustering)

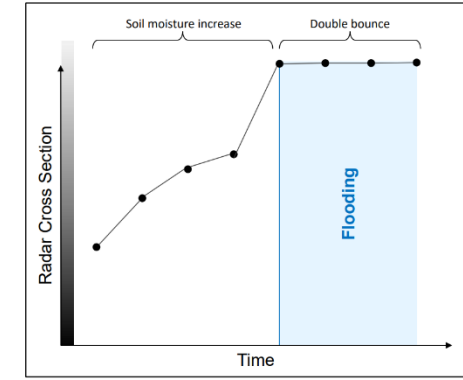
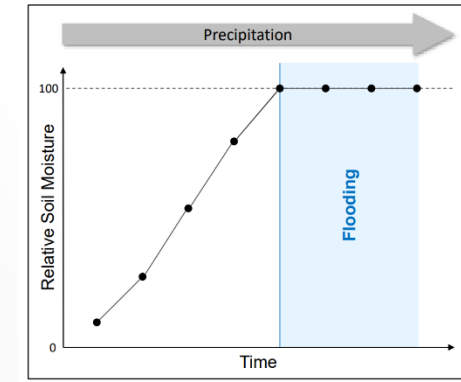
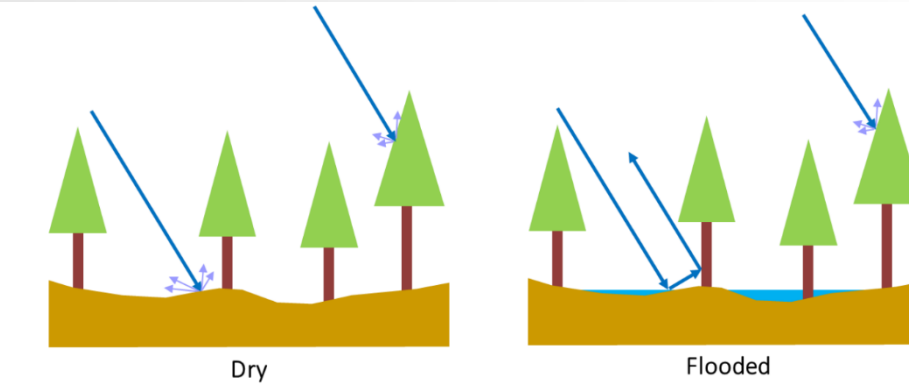


OPEN LANDS

- As precipitation increases, soil moisture increases monotonically up to a saturation point



FLOODING UNDER VEGETATION CANOPIES



FLOODING IN CROP LANDS

